Biogeochemical processes are altered by non-conservative mixing at stream confluences

Stephen Plont[1], Erin Hotchkiss[1], and Durelle Scott[2]

[1]Virginia Tech
[2]Virginia Polytechnic Institute and State University

December 8, 2022

Abstract

Stream confluences are ubiquitous interfaces in freshwater networks and serve as junctions of previously independent landscapes. However, few studies have investigated how confluences influence transport, mixing, and fate of organic matter and inorganic nutrients at the scale of river networks. To understand how network biogeochemical fluxes may be altered by confluences, we conducted two sampling campaigns at five confluences in summer and fall 2021 spanning the extent of a mixed land use stream network. We sampled the confluence mainstem and tributary reaches as well as throughout the mixing zone downstream. We predicted that biologically reactive solutes would mix non-conservatively downstream of confluences and that alterations to downstream biogeochemistry would be driven by differences in chemistry and size of the tributary and upstream reaches. In our study, confluences were geomorphically distinct downstream compared to reaches upstream of the confluence. Dissolved organic matter and nutrients mixed non-conservatively downstream of the five confluences. Biogeochemical patterns downstream of confluences were only partially explained by contributing reach chemistry and drainage area. We found that the relationship between geomorphic variability, water residence time, and microbial respiration differed between reaches upstream and downstream of confluences. The lack of explanatory power from network-scale drivers suggests that non-conservative mixing downstream of confluences may be driven by biogeochemical processes within the confluence mixing zone. The unique geomorphology, non-conservative biogeochemistry, and ubiquity of confluences highlights a need to account for the distinct functional role of confluences in water resource management in freshwater networks.

Hosted file

`essoar.10512986.1.docx` available at https://authorea.com/users/549918/articles/611615-biogeochemical-processes-are-altered-by-non-conservative-mixing-at-stream-confluences

Biogeochemical processes are altered by non-conservative mixing at stream confluences

Stephen Plont[1*], Durelle T. Scott[2], Erin R. Hotchkiss[1]

[1] Department of Biological Sciences, Virginia Polytechnic Institute and State University, Blacksburg, VA, 24061 USA

[2] Department of Biological Systems Engineering, Virginia Polytechnic Institute and State University, Blacksburg, VA, 24061 USA

*Corresponding author: Stephen Plont (stephenplont@gmail.com), ORCID 0000-0001-8477-3622

Durelle T. Scott, dscott@vt.edu, ORCID 0000-0002-5792-789X

Erin R. Hotchkiss, ehotchkiss@vt.edu, ORCID 0000-0001-6132-9107

Key Points:

1. Stream reaches downstream of confluences are geomorphically distinct from upstream reaches and have unique biogeochemical signatures within freshwater networks.
2. Differences in upstream and tributary reach chemistry or drainage area do not explain non-conservative mixing of biologically reactive solutes at confluences.
3. Confluence geomorphic heterogeneity and changes to water residence time downstream may drive differences in biogeochemical processes in confluence mixing zones.

Abstract

Stream confluences are ubiquitous interfaces in freshwater networks and serve as junctions of previously independent landscapes. However, few studies have investigated how confluences influence transport, mixing, and fate of organic matter and inorganic nutrients at the scale of river networks. To understand how network biogeochemical fluxes may be altered by confluences, we conducted two sampling campaigns at five confluences in summer and fall 2021 spanning the extent of a mixed land use stream network. We sampled the confluence mainstem and tributary reaches as well as throughout the mixing zone downstream. We predicted that biologically reactive solutes would mix non-conservatively downstream of confluences and that alterations to downstream biogeochemistry would be driven by differences in chemistry and size of the tributary and upstream reaches. In our study, confluences were geomorphically distinct downstream compared to reaches upstream of the confluence. Dissolved organic matter and nutrients mixed non-conservatively downstream of the five confluences. Biogeochemical patterns downstream of confluences were only partially explained by contributing reach chemistry and drainage area. We found that the relationship between geomorphic variability, water residence time, and microbial respiration differed between reaches upstream and downstream of confluences.

The lack of explanatory power from network-scale drivers suggests that non-conservative mixing downstream of confluences may be driven by biogeochemical processes within the confluence mixing zone. The unique geomorphology, non-conservative biogeochemistry, and ubiquity of confluences highlights a need to account for the distinct functional role of confluences in water resource management in freshwater networks.

Plain Language Summary

Stream confluences are features fundamental to the structure of freshwater networks and are often sites of physical disturbance along stream reaches. Confluences are junctions where streams draining different landscapes meet and mix, which may alter how organic matter and nutrients move and cycle throughout streams and rivers. To understand how water chemistry and microbial respiration may be altered by confluences, we sampled the upstream and downstream reaches of five confluences across a mixed land use stream network. We found that organic matter and nutrients mixed non-conservatively downstream of confluences and that alterations to downstream water chemistry and microbial respiration could not be explained by differences in chemistry and size of the tributary and upstream reaches. Confluences in our study were geomorphically distinct downstream, and the relationship between geomorphic heterogeneity, how quickly water moved, and microbial respiration differed between reaches upstream and downstream of confluences. Our findings suggest that localized differences in the physical environment downstream of confluences may be important drivers of altered biogeochemistry resulting from mixing at confluences. The prevalence of confluences and their potential impacts on the structure and function of aquatic ecosystems highlights a need to understand the role of stream confluences within landscapes.

Introduction

River networks receive and transform a diversity of material inputs from the landscapes they drain (Hynes, 1975; Vannote et al., 1980). Streams within larger river networks drain heterogenous landscapes that can vary in geomorphology and land cover, resulting in distinct biogeochemical signatures and reaction rates (Abbott et al., 2016; Mulholland et al., 2008). Furthermore, stream size and position within a river network can influence in-stream processing and downstream transport of organic matter (OM) and nutrients (Bertuzzo et al., 2017; Helton et al., 2018). While ongoing research is building a robust understanding of how streams transport and transform OM and inorganic nutrients throughout river networks (Ensign & Doyle, 2006; Koenig et al., 2019; Raymond et al., 2016), our perception of network-scale patterns in biogeochemical cycles typically ignores stream confluences due to their structural and functional complexity (Benda, et al., 2004a; Fisher et al., 2004). Confluences bring together ecosystems with potentially distinct chemistries and microbial communities and may act as unique locations of biogeochemical cycling that disproportionately contribute to the transformation of OM and inorganic nutrients throughout river networks (Bernhardt et al., 2017; Krause et al., 2017).

Stream confluences are ubiquitous features in rivers networks that are often geomorphically distinct from the reaches upstream of the confluence (Benda, et al., 2004a). Increased flow from tributary inputs can influence erosion and deposition of sediment and OM at confluences, often leading to wider, deeper reaches with unique geomorphic features such as scour holes and point bars downstream of confluences (Benda, et al., 2004a; Rice et al., 2001; Rice, 2017). These geomorphic features are commonly observed downstream of confluences throughout river networks, and act as in-channel disturbances to water routing and mixing (Rhoads & Kenworthy, 1998; Rhoads, 1987). At the reach scale, changes to in-stream geomorphology that increase water residence times, such as scour pools, may lead to increased OM decomposition and nutrient removal (Catalán et al., 2016; Zarnetske et al., 2011). While the controls of in-stream geomorphology and flow conditions on carbon and nutrient cycling have been well studied, the potential effects that abrupt changes to the physical setting downstream of confluences have on the ecosystem structure and function of streams have yet to be investigated. Case studies have suggested that confluence mixing zones are unique and diverse habitats for macroinvertebrates and fish (Fernandes et al., 2004; Rice et al., 2001). However, the influence of confluences and associated increase in geomorphic heterogeneity on the transport, mixing, and fates of OM and nutrients downstream are poorly understood.

To examine how biogeochemical fluxes are altered at confluences, we must first constrain how the solutes and materials being supplied by the upstream and tributary reaches drive the biogeochemical processes occurring throughout the confluence mixing zone. Across a river network, tributary chemistry and flow contribution can dictate the relative influence of specific tributaries on downstream patterns of OM and inorganic nutrient export (Creed et al., 2015; McGuire et al., 2014). For example, larger and more chemically-distinct tributaries should have greater leverage over biogeochemical patterns downstream of confluences (Abbott et al., 2018; Shogren et al., 2022). However, variation in physicochemistry (e.g., pH, turbidity, temperature, and dissolved oxygen) as well as differences between OM and inorganic nutrient sources between the contributing streams may stimulate or suppress biogeochemical processes in confluence mixing zones, resulting in non-conservative mixing patterns downstream of confluences that are not explained by upstream and tributary contributions alone (Fisher et al., 2004; Schemel et al., 2000). The mixing of microbial communities and OM sources at confluences may increase microbial metabolism downstream of confluences (Farjalla, 2014; Mansour et al., 2018; Ward et al., 2019). High inputs from tributaries can alleviate nutrient limitations of microbial processes and may explain observed increases in primary and secondary production downstream of confluences (Kiffney et al., 2006; Wipfli & Gregovich, 2002). Few studies have tested proposed drivers of non-conservative mixing to assess potentially distinct biogeochemical patterns downstream of confluences. Additionally, biogeochemical and ecological confluence studies are typically limited to case studies at confluences with contrasting inputs from the tributary and mainstem reaches (e.g., acid mine drainage, point source pollution, blackwater tributaries

to the Amazon River; Abarca et al., 2017; Schemel et al., 2006; Ward et al., 2016), or studies that attribute observed biogeochemical or ecological patterns to confluence-effects post-hoc (e.g., Farjalla, 2014; Kiffney et al., 2006). Overall, how differences between the chemistry and size of upstream and tributary reaches impact biogeochemical processes in the confluence mixing zone and may explain non-conservative mixing of reactive solutes downstream of confluences remains understudied (Fisher et al., 2004; Ward et al., 2019).

The degree to which ecosystem structure and function is altered within and downstream of a confluence should be linked to geomorphic variation, the materials supplied by upstream contributing reaches, and the relative contribution of each of those reaches. To quantify confluence effects on downstream biogeochemistry, we characterized the geomorphology, hydrology, water chemistry, and microbial respiration in reaches above and below the mixing zone of five confluences in a mixed-use landscape in southwest Virginia. These five confluences were located along the mainstem of the same river network and spanned a range of tributary size and agricultural, urbanized, and forested land cover. Our objectives were to (1) assess how confluences alter the transport, mixing, and fate of OM and nutrients within river networks and (2) identify drivers of non-conservative biogeochemical patterns downstream of confluences. We used differences in conservative and biologically reactive parameters to characterize which confluences mixed non-conservatively in ways we could not predict downstream biogeochemistry from the contributing reaches. We hypothesized that differences in tributary size and chemistry, in addition to the distinct morphology of mixing zones, would either stimulate or suppress biogeochemical processes at confluences in ways that could not be predicted from stream reach measurements alone.

2. Methods

2.1. Site Descriptions and Confluence Mapping

We conducted this study in the Tom's Creek catchment, a 104 km^2 watershed located near Blacksburg, VA, USA (37.20001, -80.56407) from June to November 2021. Tom's Creek and its tributaries drain a mixed-use landscape (20.3% agricultural, 12.7% developed, 67% forested at the outlet) with much of the more anthropogenic land in the southern portion of the catchment along the north-facing slopes (Figure 1). The northern portion of the catchment drains the Jefferson National Forest, a Southern Appalachian deciduous forest. Portions of the Tom's Creek catchment were sites of coal and slate mining in the early to mid-1900's, while more recent anthropogenic activity in the watershed has been focused around lower-density development and pasture-based agriculture. For our study, we selected five confluences along the Tom's Creek mainstem from its headwaters to above its confluence with the New River. These confluences spanned a range of tributary sizes and watershed land use (Table 1).

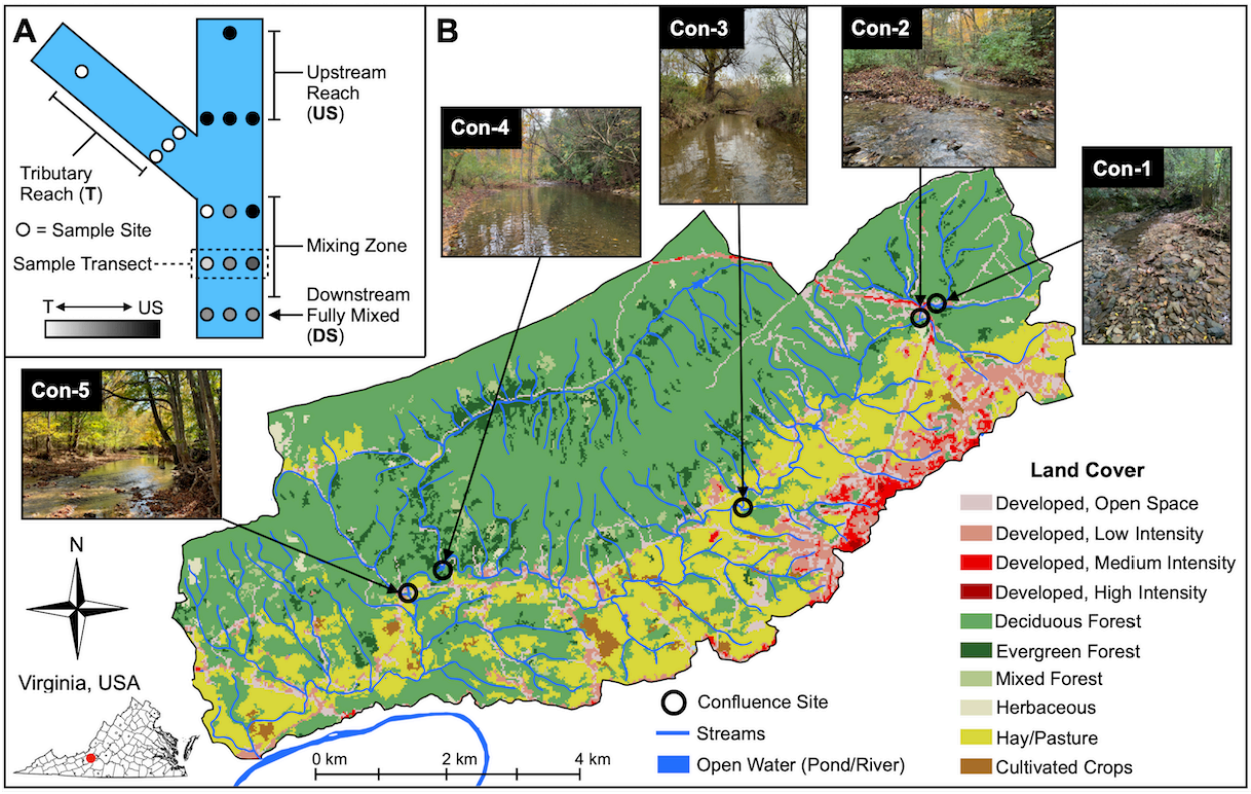

Figure 1: (A) Sampling schematic for each confluence. Each circle represents a sample site in either the upstream reach (US), the tributary reach (T), the mixing zone downstream of the confluence, or the downstream location where the tributary and upstream are fully mixed (DS). The shading of points represents the relative contribution of upstream (black) and tributary (white) to the sample site as determined by specific conductivity measurements at each sample site. (B) Land use map for the Tom's Creek catchment in Blacksburg, VA, USA. Circles indicate the location of each of the five confluences along the mainstem of the network. Tom's Creek flows from East (right of map) to West (left of map). Land cover data were retrieved from the US Geological Survey's 2011 National Land Cover Database (US Geological Survey, 2011).

To obtain drainage area and land use information, we delineated sub-watersheds for each upstream and tributary reach using the location of the near-confluence sampling transects along each contributing reach as the pour point. Using GIS software (ESRI ArcGIS v.10.7), we created flow direction and accumulation layers from a digital elevation model (DEM) used to estimate drainage (Environmental Systems Research Institute, 2022). We used the DEM derived from the 2018 Virginia FEMA NRCS South Central LiDAR Project and hosted by the Virginia Geographic Information Network (U.S. Geological Survey, 2019). We used land cover data from the U.S. Geological Survey's 2011 National Land

Cover Database to calculate forested (%FOR), agricultural (%AGR), and developed or urbanized (%URB) land use percentages for each sub-watershed (U.S. Geological Survey, 2011).

Table 1: Drainage area (km^2) and percent land cover for the sub-watersheds of each upstream (US) and tributary (T) reach contributing to each confluence. Percent forested (%FOR), agriculture (%AGR), and developed (%URB) land cover were retrieved from the US Geological Survey's 2011 National Land Cover Database (US Geological Survey, 2011).

Confluence	**Reach**	**Drainage Area (km^2)**	**%FOR**	**%AGR**	**%**
Tom's Creek-Coal Hollow Bank Creek (Con-1)	US	1.09	94.8	0.0	5.
	T	0.89	87.6	1.0	11
Tom's Creek-Brown Green Creek (Con-2)	US	3.23	89.7	0.3	10
	T	1.71	20.2	37.6	42
Tom's Creek-Heritage Park (Con-3)	US	11.2	57.6	21.2	21
	T	0.9	19.8	21.0	59
Tom's Creek-Poverty Creek (Con-4)	US	20.3	53.3	26.8	19
	T	8.93	96.7	1.0	2.
Tom's Creek-Lick Run (Con-5)	US	29.6	66.6	18.8	14
	T	2.31	90.9	4.2	4.

We recorded channel geomorphic features (e.g., scour holes, incised banks, depositional bars) at and downstream of each confluence. The Tom's Creek-Coal Bank Hollow Creek confluence (Con-1), the furthest upstream confluence along Tom's Creek with continuous flow, has large colluvial deposits at the junction of the tributary with the Tom's Creek mainstem, making it difficult to define a specific confluence point. The Tom's Creek-Brown Green Creek confluence (Con-2) has two logjams in the confluence mixing zone approximately 10 meters and 100 meters downstream of the confluence. These logjams have led to water stagnation in deep pools and accumulation of leaf litter and sediments. The tributary of the Tom's Creek-Heritage Park confluence (Con-3) is smaller than the mainstem compared to the tributaries at Con-1 and Con-2. However, scour hole, depositional bars, and incised banks were observed within the mixing zone of the confluence. Immediately downstream of the Tom's Creek-Poverty Creek confluence (Con-4), there is a large scour hole approximately 12 meters wide by 10 meters long. Lastly, the Tom's Creek-Lick Run confluence (Con-5), similar to Con-3, has a small tributary relative to the mainstem, but features incised banks and deep scour holes downstream of the confluence.

To test how confluences affect the mixing of water and solutes downstream, we mapped the physical and hydrologic setting in upstream and tributary reaches as well as the mixing zone reach downstream of each of our study confluences. We used specific conductivity measurements (SpC, µS/cm, YSI ProSolo) as a conservative tracer to assess how the tributary and upstream reaches mix down-

stream of their confluence (Figure 1A). Upstream and tributary SpC differed from 12 to 434 µS/cm at a single confluence (Table 2). We measured SpC in transects throughout the mixing zone downstream of the confluence until we reached a downstream point where SpC was equal (+/- 1 µS/cm) across the transect (i.e., where the downstream reach was fully mixed), and used these data to establish three sampling transects along each downstream reach: one transect where the stream was fully mixed and two transects within the confluence mixing zone (Figure 1A). Within each transect, we selected three sampling sites: near the left and right banks and either along the mixing boundary determined by changes in specific conductivity (for the mixing zone transects) or in the middle of the transect (for fully mixed transects). We also chose two sampling locations in each of the tributary and upstream mainstem reaches; one transect with three sampling sites close to the confluence to assess lateral heterogeneity in our reaches not associated with confluence mixing and one single (not transect) mid-channel sampling site further upstream to assess longitudinal variability along each of these reaches (Figure 1A). Along each upstream, tributary, and downstream reach, we conducted conservative tracer pulse additions of NaCl to measure velocity (u, m/min) and discharge (Q, L/s; Table 2). Reach lengths for solute pulse tracer additions ranged from 100 to 300 m and varied depending on mixing and site access for the upstream and tributary reaches. Downstream reach lengths were constrained to the extent of the confluence mixing zone, which was 100 to 125 m across the five confluences. To compare differences in water residence time between the upstream, tributary, and downstream reaches of each confluence, we calculated a reach-normalized water residence time using a reach length of 100 m (WRT_{100m}, min). NaCl additions were conducted at a confluence within 3 days after June and October samplings to avoid sample contamination while still achieving a representative measure of flow for each reach at a given confluence. In October, we also measured wetted channel width (w, m) and depth (z, m) along our focal and additional transects every 5 to 25 meters along each study reach.

Table 2: Discharge (Q; L/s), velocity (u; m/min), reach-normalized water residence time (WRT_{100m}; min), and specific conductivity (SpC; µS/cm) for the upstream (US), tributary (T), and downstream (DS; after the contributing reaches have fully mixed) reaches of each confluence for summer (Su) and fall (F) 2021 in Tom's Creek, VA.

Confluence	**Reach**	**Q (L/s)**	***u* (m/min)**	**WRT_{100m} (min)**	**SpC (µS/cm)**			
		Su	**F**	**Su**	**F**	**Su**	**F**	**Su**
Con-1	US	2.0	2.2	0.78	0.96	128.2	104.5	131
	T	0.1	0.2	0.42	0.30	238.1	333.3	142
	DS	2.2	2.4	0.54	0.38	185.2	266.6	131
Con-2	US	9.5	16.9	1.87	1.50	53.3	66.8	258
	T	18.8	30.0	5.37	3.14	18.6	31.8	494
	DS	28.7	49.1	1.67	1.33	59.9	75.2	413
Con-3	US	64.2	126.8	2.24	4.27	44.6	23.4	540

Confluence	Reach	Q (L/s)	u (m/min)	WRT_{100m} (min)	SpC (µS/cm)			
	T	25.2	38.4	6.02	4.07	16.6	24.6	585
	DS	92.3	169.5	3.57	4.67	28.0	21.4	560
Con-4	US	169.7	265.1	7.79	7.52	12.8	13.3	551
	T	22.7	42.5	1.09	2.75	91.6	36.4	117
	DS	195.2	314.5	7.10	6.42	14.1	15.6	500
Con-5	US	265.6	299.4	9.25	7.38	10.8	13.6	498
	T	18.2	17.0	2.03	1.01	49.3	99.4	201
	DS	291.0	325.9	8.45	6.99	11.8	14.3	477

2.2 Synoptic Sampling

Over the course of two weeks in both June and October 2021, we collected samples for biogeochemical analyses and took *in situ* measurements at our five confluence sites. At each confluence, we collected triplicate water samples from three sites along each sampling transect downstream of the confluence and at two sites along the mainstem and tributary reaches upstream of the confluence (Figure 1). We used handheld sensors in the field to measure turbidity (NTU, Turner Designs AquaFluor), dissolved oxygen (mg/L, YSI ProSolo), temperature (°C, YSI ProSolo), and SpC (µS/cm, YSI ProSolo). We filtered samples for DOC concentration through pre-ashed GF/F filters into acid-washed and ashed 40-mL amber borosilicate vials. After filtering, we acidified each DOC sample by adding a 2% (by volume) aliquot of 2N HCl and refrigerated them until analysis on a Elementar varioTOC Analyzer (as non-purgeable organic carbon, NPOC, as in Plont et al., 2022). Samples for dissolved OM (DOM) optical properties were filtered into amber vials until no headspace remained, not acidified, and refrigerated until analysis. We filtered nutrient samples through 0.22 µm PES filters into acid-washed 60-mL HDPE bottles, which we froze at -20°C until analysis. We analyzed nutrient samples for NH_4^+-N using the phenolhypochlorite method (Solórzano, 1969), NO_3^--N using the cadmium reduction method (APHA 1998), and SRP using the ascorbic acid method (Murphy & Riley, 1962) on a Lachat Flow Injection Autoanalyzer (Lachet Instruments).

1. **Dissolved Organic Matter Optical Properties**

We analyzed samples collected throughout each confluence for DOM optical properties via absorbance and fluorescence spectroscopy. Ultraviolet (UV)–visible absorbance spectra from 220 to 800 nm were collected using quartz cuvettes with a 1 cm path length on a Shimadzu UV 1800 spectrophotometer (Shimadzu Scientific Instruments). Excitation-emission matrices (EEMs) were measured over excitation wavelengths of 250–450 nm and emission wavelengths of 320–550 nm on a Horiba Aqualog fluorometer (Horiba Scientific). E-Pure water (18 MΩ, Barnstead E-Pure system) was used as a blank and cuvettes were triplicate rinsed with E-Pure water and then rinsed with sample water between readings. Instrument-specific excitation and emission corrections were applied to each EEMs to account for Raman scattering and the inner-filter effect (Cory

et al., 2010). Fluorescence intensities from corrected-sample EEMs were then converted to Raman units (Stedmon & Bro, 2008).

Using EEMs and UV–visible absorbance spectra, we calculated DOM quality indices for each sample. Specific UV absorbance at 254 nm ($SUVA_{254}$) was calculated using absorbance readings at 254 nm normalized for path length (m) and DOC concentration (mg/L). Higher $SUVA_{254}$ values are associated with higher aromaticity of DOM (Weishaar et al., 2003). Following Coble (1996), we used EEM peak C (ex 365/em 466; a proxy for humic-like, often terrestrially-derived fluorescent DOM), EEM peak T (ex 285/em 344; a proxy for protein-like, often microbially-derived fluorescent DOM) and the ratio of EEM peak C to EEM peak T (C:T) to discuss differences in relative DOM structure and source between sites.

1. **Water Column Microbial Respiration Assays**

We estimated water column microbial respiration across each of our confluences using short-term laboratory incubations (e.g., Ward et al., 2019). We filled six acid-washed 300-mL amber PET Winkler titration bottles (Environmental Express) with stream water at each confluence sampling site (Figure 1A). Each Winkler bottle was rinsed with stream water before it was filled and capped underwater with no headspace. Capped Winkler bottles were stored in coolers to avoid light exposure and allowed to sit for approximately one hour for the water temperature inside each bottle to equilibrate to ambient air temperatures (~20°C). After one hour, we sacrificially sampled three bottles from each site and measured initial dissolved oxygen (DO) concentrations. The remaining bottles were transported back to the laboratory in coolers, submerged in water to below their lids to maintain temperatures ~20°C, and incubated in the dark for 4 days. After 4 days, we measured final DO concentrations.

We calculated potential rates of water column microbial respiration (k_{DO}, day^{-1}) based on first-order reaction kinetics:

$O_t = O_o e^{-k_{\mathrm{DO}} t}$ (Equation 1)

where O_o and O_t are DO concentrations (mg/L) at the start and end of the incubation period t (days), respectively. We used a Bayesian inverse modeling approach to estimate the posterior probability distributions for k_{DO} at each site that best predicted measured O_t (modified from Hotchkiss et al., 2014). We used a nominally-informative, normally distributed prior for k_{DO} with a mean of 0.05 day^{-1} and a standard deviation of 0.50 day^{-1}. We simulated the k_{DO} posterior probability distributions using the *rjags* package and Markov chain Monte Carlo sampling (R Core Team, 2022). For each model, we ran 50,000 iterations with 1,000 burn-in steps and 49,000 saved steps using three different starting values sampled from our prior distribution. After estimating k_{DO} posterior means and credible intervals, we compared measured versus modeled O_t to test model fits (Supplementary Figure 1). We assessed model convergence using the Gelman-Rubin convergence diagnostic (*Rhat*) and established a quality-check threshold

that would remove sites from further analysis with *Rhat* values larger than 1.1 or with unreasonable k_{DO} (i.e., negative k_{DO}) (Gelman & Rubin, 1992).

1. **Testing for Non-Conservative Mixing of Bioreactive Parameters**

An overarching assumption in most freshwater network biogeochemical measurements and models is that tributaries mix conservatively with the mainstem reach at confluences. That is, the value of a parameter (e.g., SpC, NO_3^-) downstream of a confluence should be equal to parameter values in the upstream (US) and tributary (T) reaches scaled proportionally to flow in each reach. However, changes to the biotic and abiotic setting within and downstream of confluences may enhance or suppress biogeochemical processes and lead to non-conservative mixing of OM and nutrients. To test for potential non-conservative mixing of bioreactive parameters (DOC, NO_3, NH_4, SRP, $SUVA_{254}$, Peak C, Peak T, C:T, and k_{DO}) downstream of a confluence, we compared measured values from sites downstream of a confluence at the point where the tributary and mainstem have fully mixed (DS) with modeled values derived from a mixing model that assumes conservative mixing of US and T (Equation 2). The mass-balance equation that governs the confluence mixing model is:

$$C_{DS,\ mod} = \frac{C_{\mathrm{US}}Q_{\mathrm{US}}+C_T Q_T}{Q_{\mathrm{DS}}} \text{ (Equation 2)}$$

We calculated modeled DS parameter values ($C_{DS,\ mod}$) for SpC and all bioreactive parameters. C_{US} and C_T refer to the measured US and T parameter values, respectively. Q_{US}, Q_T, and Q_{DS} are discharge in the US, T, and DS reach of a confluence. We assumed no gaining or losing along DS reaches and checked this assumption by comparing the sum of Q_{US} and Q_T with Q_{DS}. Across both sampling campaigns at all five confluences, $Q_{DS} = Q_{US} + Q_T$ (+/- 2 to 9%), which is within the margins of error in discharge estimates, and we thus excluded this small potential water gain or loss downstream of the confluence from our mass balance calculations.

To test for non-conservative behavior of a bioreactive parameter downstream of a confluence, we calculated the relative difference between measured and modeled DS values (Equation 3):

$$\mathrm{pdiff}_{\mathrm{DS}} = \frac{C_{DS,meas}-C_{DS,\ mod}}{C_{DS,\ mod}} * 100 \text{ (Equation 3)}$$

$pdiff_{DS}$ is the percent difference between the parameter value measured at the fully mixed site downstream of a confluence ($C_{DS,\ meas}$) and the modeled downstream parameter value calculated using Equation 2 ($C_{DS,\ mod}$). If $pdiff_{DS} = 0$, then the downstream value can be explained by conservative mixing of the US and T reaches. If $pdiff_{DS}$ is greater or less than 0, then there is a net increase or decrease in the downstream parameter that suggests the confluence mixing zone is contributing to non-conservative behavior of the parameter through enhancement ($pdiff_{DS} > 0$) or suppression ($pdiff_{DS} < 0$) of biogeochemical reactions.

We tested the potential role of different hydrologic and biogeochemical drivers on non-conservative mixing of bioreactive parameters downstream of confluences.

To assess differences in contributing reach chemistry as a potential driver of non-conservative mixing, we calculated the relative difference of bioreactive parameters between the T and US reach ($pdiff_{T:US}$) as the percent difference between a bioreactive parameter in the tributary (C_T) and upstream (C_{US}) of a confluence (Schemel et al. 2000):

$$\text{pdiff}_{T:US} = \frac{C_T - C_{\text{US}}}{C_{\text{US}}} * 100 \text{ (Equation 4)}$$

To test the role of differences in drainage area as a predicted control on non-conservative mixing, we calculated a ratio of T and US drainage areas (DA_T:DA_{US}).

Lastly, we explored how geomorphic and hydrologic change associated with confluences contributed to the stimulation or suppression of biogeochemical processes (in this case: water column microbial respiration, k_{DO}). We calculated the coefficient of variation for wetted width (w_{cv}) across the US and DS reach of each confluence as a metric of reach-scale geomorphic variability. We used $\text{WRT}_{100\text{m}}$ as a potential hydrologic driver of non-conservative biogeochemical behavior. We assessed the relationship between both w_{cv} and $\text{WRT}_{100\text{m}}$ with the mean of all k_{DO} measurements across each US and DS reach ($k_{DO\text{-}reach}$, day^{-1}) to include k_{DO} measurements from mixing zones and fully mixed transects along DS reaches.

1. **Statistical Analysis**

At each confluence, we used a two-way analysis of variance (ANOVA) to assess differences Q, u, SpC, and all bioreactive parameters between US and DS and between the summer and fall. Reach and sampling campaign were treated as fixed effects and we tested for significant interactions between reach and sampling campaign for each parameter at each confluence. For w and z surveys, we used a one-way ANOVA to test for differences in w and z upstream and downstream at each confluence. To evaluate the relationship between $pdiff_{DS}$ and $pdiff_{T:US}$ and between $pdiff_{DS}$ and DA_T:DA_{US}., we used generalized linear models. We used coefficients of determination of these linear models (R^2) to assess the degree to which $pdiff_{T:US}$ or DA_T:DA_{US} explained the variability in $pdiff_{DS}$ for a given parameter. We also used the magnitude and directionality of the slope from these linear models to interpret whether a given bioreactive parameter conservatively (i.e., slope = 0) or non-conservatively (i.e., slope is positive or negative) mixed downstream of a confluence. Lastly, we used generalized linear models to evaluate the relationship between $k_{DO\text{-}reach}$, w_{cv}, and $\text{WRT}_{100\text{m}}$. For all statistical analyses, we assigned a significance level of alpha = 0.05. All statistical analyses were conducted using R (R Core Team, 2022).

Results

1. **Confluence Hydrology and Geomorphology**

Under baseflow conditions, hydrologic parameters differed across upstream (US), tributary (T), and downstream (DS) reaches and among confluences, but did

not vary between sampling campaigns. Discharge (Q) and velocity (u) in all US reaches in summer did not differ from all US reaches in fall ($p = 0.22$ and $p = 0.09$, respectively, Table 2). Q in all DS reaches was equal to the sum of the T and US reaches (+/- 2 to 9%) during both sampling campaigns. Among all five confluences, T reaches contributed 5 to 67% of the flow in the DS reach. There was no consistent pattern of u downstream of a confluence within our study network.

Among all five confluences, mean channel wetted width (w) and depth (z) were different and more variable in DS reaches compared to their respective US reaches (Figure 2). The DS reaches of three of five confluences were wider than US reaches ($p < 0.001$ for Con-1, Con-2, and Con-3, respectively). The DS reach of Con-5 was narrower than upstream ($p < 0.001$), but this result may have been biased by the small number of w measurements ($n = 5$ instead of $n = 12$ to 24) along the US and DS reach due to site inaccessibility. w did not differ between the Con-4 US and DS reaches ($p = 0.15$), likely due to DS w being more variable ($w_{cv} = 29.8\%$) than US ($w_{cv} = 11.8\%$). DS reaches were also deeper than US at all confluences due to the presence of scour holes and large pools, which were only present in DS reaches (Figure 2). Confluence-derived channel features led to a maximum z along each DS reach that was approximately double that of the maximum z measured US (Figure 2).

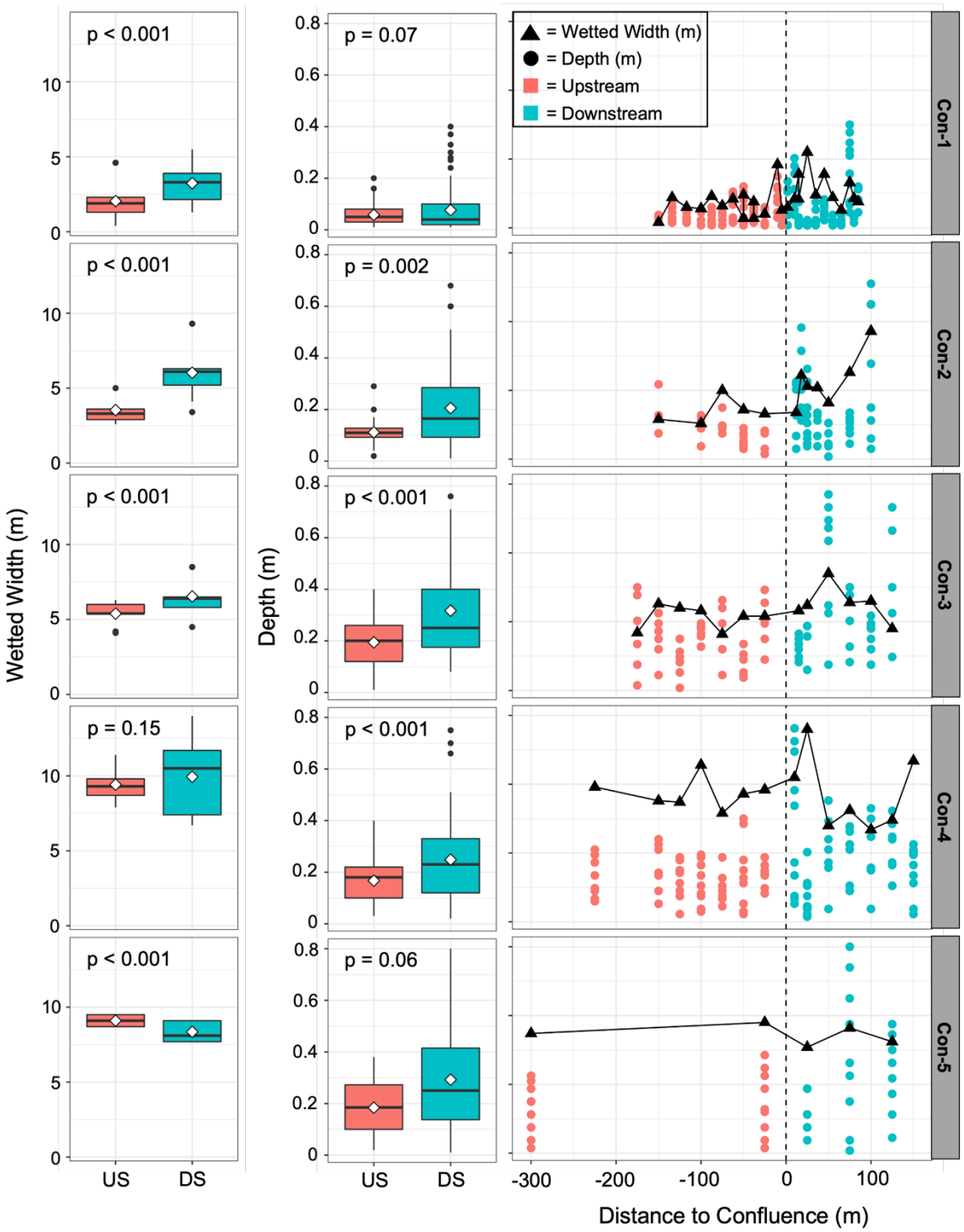
p < 0.001
p = 0.07
= Wetted Width (m)
= Depth (m)
= Upstream
= Downstream
Con-1
p < 0.001
p = 0.002
Con-2
p < 0.001
p < 0.001
Con-3
p = 0.15
p < 0.001
Con-4
p < 0.001
p = 0.06
Con-5
Wetted Width (m)
Depth (m)
US
DS
-300
-200
-100
0
100
Distance to Confluence (m)

Figure 2: Average wetted width (m) and depth (m) across each Tom's Creek confluence during our fall 2021 campaign. In the first and second column, wetted width and depth are pooled based on whether they were taken upstream of the confluence (US) or downstream of the confluence (DS). In the third column, wetted width measurements are represented as the triangles connected by the black line. Depth measurements, collected across each width transect are represented by either orange points (US) or blue points (DS). Depth and wetted width measurements in the third column are scaled based on the wetted width and depth scales in the first and second column, respectively.

1. Variability in Bioreactive Parameters Within and Across Confluences

Specific conductivity (SpC) and bioreactive parameters differed by season and between US and DS reaches at each confluence (Figure 3). SpC was the only parameter that differed between summer and fall and between US and DS at all five confluences (all p-values can be found in Supplementary Table 1). We found significant interactions between season and reach SpC at Con-2 and Con-4, which we interpreted as confluence differences being seasonally-dependent. We observed seasonal differences in bioreactive parameters across the five study confluences. DOC, peak C, peak T, and NO_3-N differed between summer and fall in US reaches at all confluences (Supplementary Table 1). NH_4-N differed between summer and fall in US reaches at all confluences except Con-2 (Supplementary Table 1). SRP differed between summer and fall in US reaches for all confluences except Con-1, and $SUVA_{254}$ differed between summer and fall for Con-2, Con-4, and Con-5 (Supplementary Table 1).

Differences between reaches of a confluence for a given parameter were confluence-specific; no bioreactive parameter differed between US and DS reaches at all confluences. SRP only differed between US and DS at Con-4 ($p < 0.001$). $SUVA_{254}$ differed between US and DS at Con-2 ($p = 0.019$) and Con-4 ($p = 0.008$). These differences in SRP and $SUVA_{254}$ between US and DS reaches depended on season ($p < 0.001$ for SRP at Con-4, $p = 0.017$ and $p = 0.028$ for $SUVA_{254}$ at Con-2 and Con-4, respectively). NO_3-N differed between US and DS at Con-1 ($p = 0.001$), Con-2 ($p < 0.001$), and Con-3 ($p = 0.011$). Differences in NO_3-N between US and DS in the confluences higher in the network (i.e., Con-1, Con-2, and Con-3) were driven by tributary reaches acting as point sources of high NO_3-N inputs to the network.

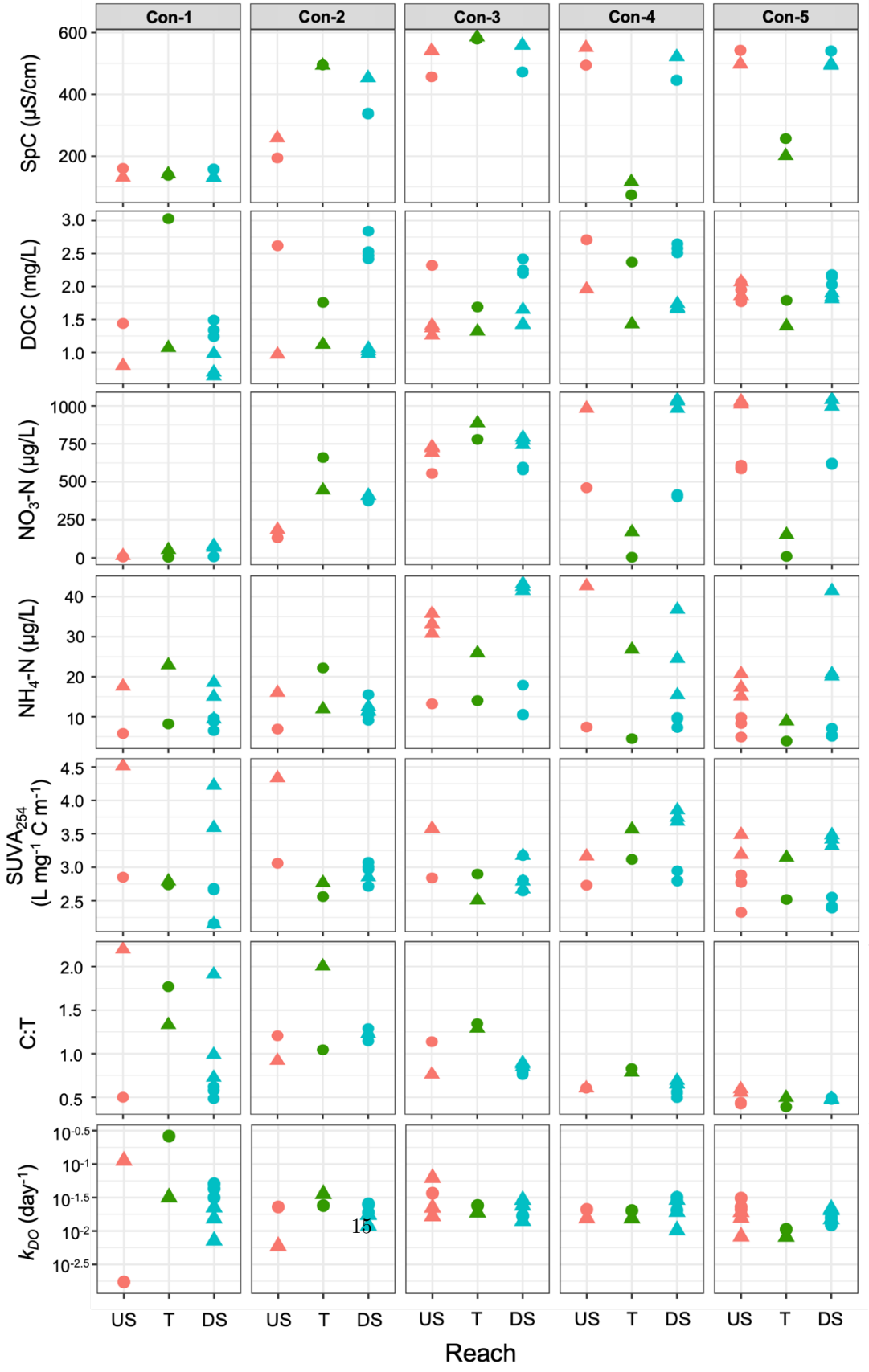
Con-1
Con-2
Con-3
Con-4
Con-5
SpC (µS/cm)
DOC (mg/L)
NO3-N (µg/L)
NH4-N (µg/L)
SUVA254 (L mg-1 C m-1)
C:T
kDO (day-1)
US
T
DS
Reach

Figure 3: Specific conductivity (µS/cm), dissolved organic carbon (DOC, mg/L), nitrate (NO_3-N, µg/L), ammonium (NH_4-N, µg/L), specific ultraviolet absorbance of DOC at 254 nm ($SUVA_{254}$, L mg^{-1} C m^{-1}), peak C: peak T (C:T), and microbial respiration rate (k_{DO}) in the upstream (US), tributary (T), and downstream (DS) reaches of the five confluences. Points represent mean values of three replicate samples taken at each site. Triangles are values from summer 2021 and circles are values from fall 2021.

1. Mixing Behavior and Differences in Contributing Reach Chemistry

Bioreactive parameters downstream of confluences responded differently to mixing of US and T inputs. For SpC, the conservative parameter used to characterize solute inputs and mixing not altered by biogeochemical transformations, $pdiff_{DS}$ ranged from -2 to 1% (Figure 4B), which confirmed that DS SpC was a flow-weighted, conservative mixture of T and US, and could therefore be used to compare potential non-conservative mixing of bioreactive solutes from contributing reaches. All bioreactive parameters had larger $pdiff_{DS}$ ranges than SpC, indicating that DS parameter values cannot be predicted by conservative mixing of US and T reaches alone. k_{DO} at DS sites did not behave conservatively, with $pdiff_{DS}$ ranging from -93 to 159%, indicating both stimulation and suppression of microbial respiration at confluences (Figure 4C). DOC, $SUVA_{254}$, and C:T spanned similar ranges of $pdiff_{DS}$ (-21 to 37%, -51 to 20%, and -66 to 16%, respectively) with more sites downstream of confluences having negative $pdiff_{DS}$ for $SUVA_{254}$ and C:T in summer and fall (54% and 62% of sites, respectively). Negative $SUVA_{254}$ and C:T $pdiff_{DS}$ indicated a less aromatic, more microbially-derived DOM signature downstream of confluences than would be predicted from the upstream and tributary DOM inputs to the confluence. Across the Tom's Creek network, $pdiff_{DS}$ for NO_3-N, NH_4-N, and SRP were both negative and positive (-20 to 443%, -52 to 139%, and -62 to 60%, respectively).

Differences in T and US bioreactive parameter values ($pdiff_{T:US}$) partially explained non-conservative mixing downstream of confluences. SpC differed between the US and T reaches at all confluences: $pdiff_{T:US}$ ranged from 8 to 155%. As $pdiff_{T:US}$ increased, k_{DO} was suppressed downstream (Figure 4C). Confluences with higher $pdiff_{T:US}$ were a net sink of DOC (Figure 4D), and had lower $SUVA_{254}$ downstream that was not explained by conservative mixing (Figure 4E). $pdiff_{DS}$ for NO_3-N and SRP increased as a function of $pdiff_{T:US}$, indicating that at confluences where T and US NO_3-N and SRP concentrations differed, the DS reach acted as a net source of NO_3-N and SRP (Figure 4G and 4I). These net source trends for NO_3-N and SRP were driven by two high $pdiff_{T:US}$ confluence sites. For example, NO_3-N concentrations differed 289% between the T and US reaches at Con-1 in summer, with $pdiff_{DS}$ ranging from 357 to 443% (Figure 4G). Similarly for SRP, summer $pdiff_{T:US}$ at Con-1 and fall $pdiff_{T:US}$ at Con-2 were greater than the majority of other SRP $pdiff_{T:US}$ values (276% and 120%, respectively). SRP $pdiff_{DS}$ was also higher for summer Con-1 and fall Con-2 compared to the other confluences (Figure 4I). While there were rela-

tionships between $pdiff_{T:US}$ and $pdiff_{DS}$ for several bioreactive parameters, some of the highest $pdiff_{DS}$ values occurred when parameter values in the US and T reaches were more similar (i.e., confluences with low $pdiff_{T:US}$). k_{DO} $pdiff_{DS}$ for Con-4 ranged from -34 to 88% while $pdiff_{T:US}$ for Con-4 ranged from 0.5 to 4% (Figure 4C), indicating both net stimulation and suppression of biogeochemical processes downstream of confluences with similar US and T k_{DO}.

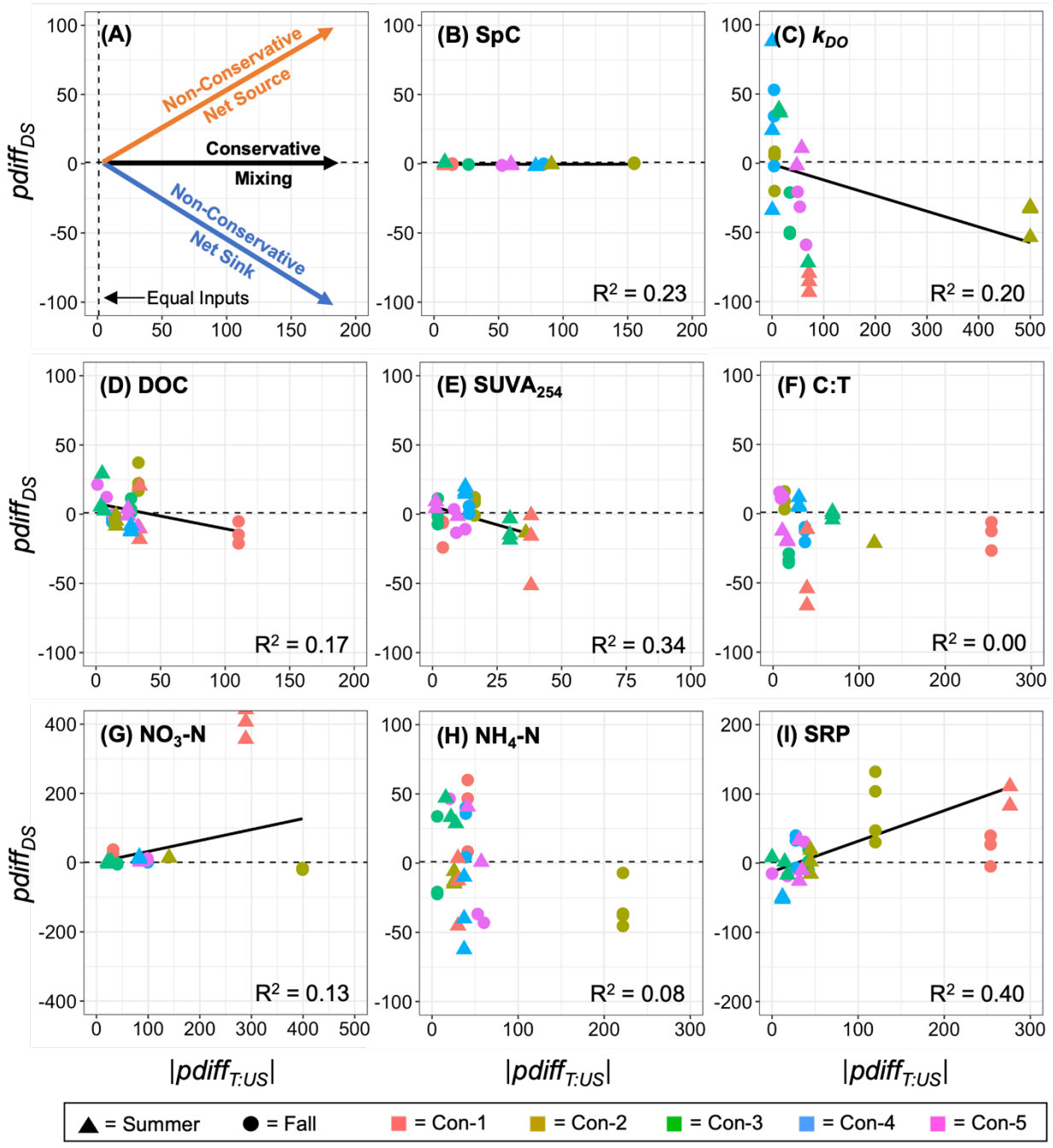

Figure 4: Percent difference in measured and modeled downstream (DS) parameter values ($pdiff_{DS}$) vs. percent difference in tributary (T) and upstream (US) inputs to each confluence ($pdiff_{T:US}$). The top left panel (A) shows po-

tential data trends and explanations as $pdiff_{T:US}$ increase. At $pdiff_{T:US} = 0$, parameter values from US and T are equal. As $pdiff_{T:US}$ increases, $pdiff_{DS}$ may (1) not change indicating conservative mixing downstream of the confluence (black arrow and dotted horizontal line), (2) increase, indicating DS reaches behave non-conservatively and are a net source (orange arrow), or (3) decrease, indicating DS reaches behave non-conservatively and are a net sink (orange arrow). Panels B through I represent $pdiff_{DS}$ vs. $pdiff_{T:US}$ for specific conductivity (SpC; B), water column microbial respiration rate (k_{DO}; C), dissolved organic carbon (DOC; D), specific ultraviolet absorbance at 254 nm ($SUVA_{254}$; E), peak C: peak T (C:T; F), nitrate (NO_3-N; G), ammonium (NH_4-N; H), and soluble reactive phosphorus (SRP; I). Linear regressions (black solid lines in data plots) are included for parameters with statistically significant relationships ($p < 0.05$). R^2 values from simple linear regressions are included for all parameters. Triangles are values from summer and circles are values from fall. Each confluence is represented by a different color.

1. Mixing Behavior and Drainage Area Ratio of Contributing Reaches

The five confluences we studied spanned a range of tributary drainage areas independent of position in the network. Drainage area ratios of tributary and upstream reaches (DA_T:DA_{US}) ranged from 0.08 to 0.82 for the five confluences (Figure 5). The two confluences highest in the network (Con-1 and Con-2) had the highest DA_T:DA_{US} (0.82 and 0.53, respectively), followed by Con-4 with a DA_T:DA_{US} of 0.44. Con-3 and Con-5 were confluences with small tributaries and both had DA_T:DA_{US} values of 0.08. Despite these low DA_T:DA_{US} values for Con-3 and Con-5, the presence of unique erosional and depositional features and resulting differences in w and z between US and DS reaches indicate that the small tributaries at Con-3 and Con-5 still lead to observable geomorphic change downstream of these confluences (Figure 2).

For bioreactive parameters other than NO_3-N and SRP, DA_T:DA_{US} did not explain non-conservative behavior downstream of confluences. When drainage areas of T and US reaches were more similar, there was a higher discrepancy between measured and modeled NO_3-N and SRP concentrations downstream of the confluence (Figure 5); $pdiff_{DS}$ of NO_3-N and SRP was positively related to DA_T:DA_{US} ($p = 0.002$ and $p = 0.006$, respectively). Confluences with low DA_T:DA_{US} mixed non-conservatively for all bioreactive parameters with $pdiff_{DS}$ between -50 and 50% and did not exhibit seasonal differences in $pdiff_{DS}$ (Figure 5). However, for confluences with higher DA_T:DA_{US}, the $pdiff_{DS}$ for k_{DO}, NO_3-N, NH_4-N, and SRP differed between summer and fall. k_{DO} $pdiff_{DS}$ shifted from net suppression downstream of the Con-1 and Con-2 in summer (-93 to -32%) to net stimulation (35 to 117% for Con-1) or a conservative mixture of the US and T (5 to 8% for Con-2) in fall (Figure 5). During both sampling campaigns, the DS reach of Con-1 was a net source of NO_3-N ($pdiff_{DS}$ from 357 to 443% in summer, 27 to 38% in fall) and SRP ($pdiff_{DS}$ from 83 to 289% in summer, -5 to 40% in fall). At Con-4, the DS reach was a net sink of SRP in summer

($pdiff_{DS}$ from -33 to -10%) and a net source in fall ($pdiff_{DS}$ from -7 to 40%). The downstream reaches of Con-1 and Con-4 were typically net sinks of NH_4-N in summer ($pdiff_{DS}$ from -45 to 4% for Con-1, -62 to -10% for Con-4) and net sources in fall (8 to 60% for Con-1, 4 to 40% for Con-4).

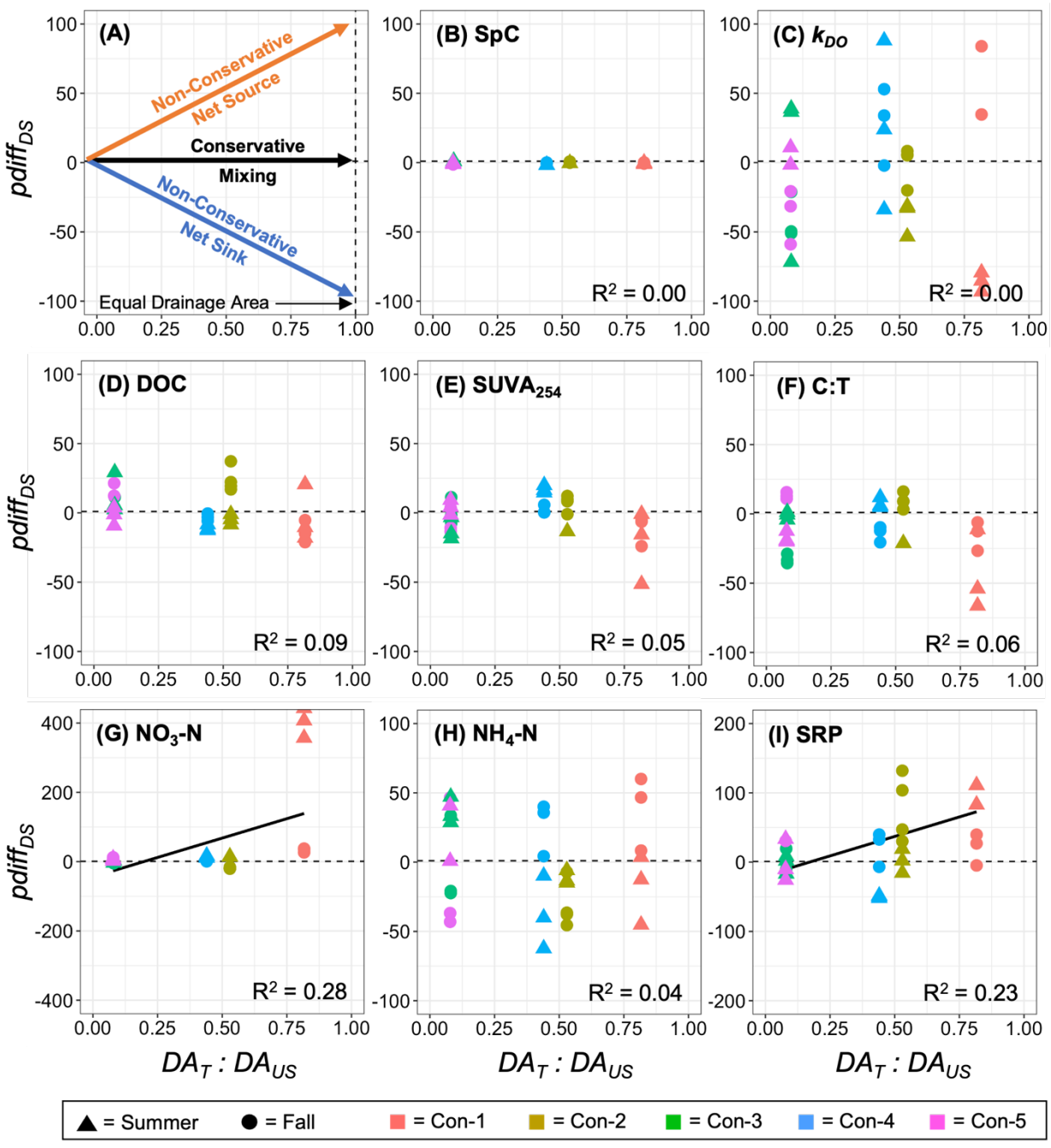

Figure 5: Percent difference in measured and modeled downstream (DS) parameter values ($pdiff_{DS}$) vs. the ratio of tributary (T) and upstream (US) subwatershed drainage areas (DA_T:DA_{US}). The top left panel (A) shows potential

data trends and their meanings as DA_T:DA_{US} increases. At DA_T:DA_{US} = 1, the drainage area of the T and US sub-watersheds are equal. As DA_T:DA_{US} increases, $pdiff_{DS}$ may (1) not change indicating conservative mixing downstream of the confluence (black arrow and dotted horizontal line), (2) increase indicating DS reaches behave non-conservatively and are a net source (orange arrow), or (3) decrease indicating DS reaches behave non-conservatively and are a net sink (orange arrow). Panels B through I represent $pdiff_{DS}$ vs. DA_T:DA_{US} for specific conductivity (SpC; B), water column microbial respiration rate (k_{DO}; C), dissolved organic carbon (DOC; D), specific ultraviolet absorbance at 254 nm ($SUVA_{254}$; E), peak C: peak T (C:T; F), nitrate (NO_3-N; G), ammonium (NH_4-N; H), and soluble reactive phosphorus (SRP; I). Linear regressions (black solid lines in data plots) are included for parameters with statistically significant relationships ($p < 0.05$). R^2 values from simple linear regressions are included for all parameters. Triangles are values from summer and circles are values from fall. Each confluence is represented by a different color.

1. Reach Geomorphology, Water Residence Time, and Reach-Scale k_{DO}

Variation in wetted width across a reach (w_{cv}) and reach-normalized water residence time (WRT_{100m}) explained patterns of $k_{DO\text{-}reach}$ across the US and DS reaches of all five confluences. Except for Con-3, WRT_{100m} was longer in DS reaches compared to their respective US reaches (Table 2, Supplementary Figure 2). Apart from Con-1, DS reaches had higher w_{cv} and were more geomorphically variable than their respective US reaches. w_{cv} of the US reaches was highest at Con-1 and decreased from higher to lower in the network (Figure 6A). w_{cv} of the DS reaches, however, was not related to network position, but instead was negatively correlated with tributary size (Supplementary Figure 3). Whether US and DS geomorphology was related to network position or tributary size was also reflected in the directionality of the relationship between w_{cv} and $k_{DO\text{-}reach}$. For US reaches of each confluence, $k_{DO\text{-}reach}$ had a negative relationship with w_{cv} ($p = 0.138$, Figure 6A), while $k_{DO\text{-}reach}$ positive relationship with w_{cv} in DS reaches ($p = 0.075$, Figure 6C). Similar to w_{cv}, $k_{DO\text{-}reach}$ had a negative relationship with WRT_{100m} in US reaches ($p = 0.090$, Figure 6B), while $k_{DO\text{-}reach}$ had a positive relationship with WRT_{100m} in DS reaches ($p = 0.041$, Figure 6D).

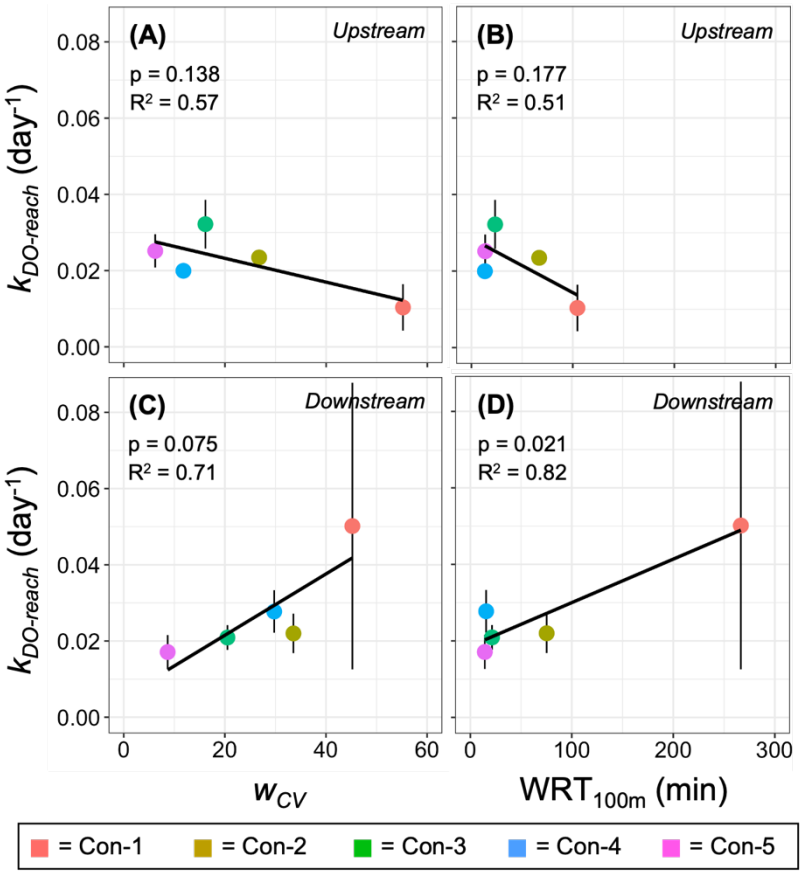

Figure 6: Reach-scale mean water column microbial respiration rate ($k_{DO\text{-}reach}$, day^{-1}) versus reach-scale coefficient of variation for wetted width (w_{cv}; left) and water residence time normalized to a 100 meter reach ($\mathrm{WRT}_{100\mathrm{m}}$, min; right) along the upstream (top) and downstream (bottom) reaches of each confluence. Vertical lines are +/- 1 standard deviation of $k_{DO\text{-}reach}$. Each confluence is represented by a different color. Black lines are linear fits of the data. R^2 values from simple linear regressions are included for all parameters.

Discussion

We characterized the physical environment and measured bioreactive parameters throughout the upstream, tributary, and downstream reaches of five confluences across a mixed land use stream network. We assessed how differences in tributary and upstream inputs and size, as well as geomorphic and hydrologic differences downstream of a confluence, predicted non-conservative mixing of bioreactive parameters at confluences. Reaches downstream of confluences were morphologically and biogeochemically distinct compared to their upstream and tributary reaches. Bioreactive parameters mixed non-conservatively down-

stream of all five confluences. Non-conservative mixing responses downstream of confluences varied among bioreactive parameters and were only partially explained by differences in contributing reach chemistry or drainage area. The lack of explanatory power of network-scale drivers suggests that stimulation or suppression of biogeochemical processes in the confluence mixing zone may contribute to non-conservative mixing patterns of bioreactive parameters downstream. Differences in geomorphic heterogeneity and water residence time between reaches upstream and downstream of confluences may drive alterations to microbial respiration in confluence mixing zones.

1. **Confluences are Geomorphic and Hydrologic Discontinuities in Stream Networks**

In our study, confluences acted as geomorphic discontinuities along the Tom's Creek network. Regardless of relative tributary size or network position, reaches downstream of confluences were wider, deeper, and had more variable channel geomorphology compared to upstream. These findings are consistent with other studies that observed confluence effects on channel geomorphology in temperate river networks (Benda et al., 2004b). Confluences that impact in-channel geomorphology downstream act as flow discontinuities in river networks and can lead to in-channel disturbance in reaches immediately upstream of confluences (Benda et al., 2004a). We observed these upstream disturbance effects at Con-1, which was the uppermost confluence in the network and had the highest DA_T:DA_{US}. The extent of geomorphic disturbance at Con-1 made identifying the point at which the tributary entered the mainstem difficult. Despite the low flow and slow velocity conditions at Con-1 during both sampling campaigns, the presence of large cobbles and woody debris in the channel, incised stream banks, and a discordant streambed downstream indicated that the physical setting of this confluence was disturbed and shaped by high peak flow events. All five confluences in our study had unique geomorphic features common in reaches downstream of confluences, such as scour holes, incised stream banks, and depositional bars of larger sediment and woody debris (Rhoads, 1987). The presence of distinct geomorphic features at confluences throughout the Tom's Creek network shows that confluence effects on ecosystem structure and function occur regardless of size or network position.

Geomorphic disturbances at confluences influence how water and materials moves and mix downstream. Geomorphic features of stream channels can alter water residence times, reactive surface area, and hydrologic exchange at the reach scale by influencing where and how water and materials move, mix, and interact with riparian and hyporheic zones (Harvey & Gooseff, 2015; Schmadel et al., 2016; Ward et al., 2012). While reach-scale velocity did not differ between reaches upstream and downstream of the five confluences, reach-normalized water residence time ($\mathrm{WRT}_{100\mathrm{m}}$) was slightly longer in downstream reaches compared with upstream reaches. Erosional and depositional features downstream of confluences can increase residence times in scour pools and play an important role in controlling downstream mixing lengths of tributary

and upstream reaches (Best, 1987; Gaudet & Roy, 1995). However, given the higher variability in width and depth downstream, the localized influence of geomorphic disturbance features within the confluence mixing zone could impact the routing and mixing of water and materials along the downstream reach beyond what can be represented by reach-scale measurements. Future work linking confluence-specific geomorphic features to the routing of water to and throughout the confluence mixing zone is needed to further elucidate how disturbances to ecosystem structure impact biogeochemical processes downstream of confluences.

1. **Biogeochemical Fluxes and Processes are Altered Downstream of Confluences**

We found evidence for both net stimulation and suppression of biogeochemical processes at confluences. Reaches downstream of confluences were net sources or sinks of OM and inorganic nutrients; DOC, NH_4-N, NO_3-N, and SRP concentrations were all higher or lower than predictions based on conservative mixing. Tributaries can supply or dilute OM and nutrient concentrations along mainstem reaches, which may increase microbial respiration and primary production downstream of confluences (Farjalla, 2014; Kiffney et al., 2006). However, our data suggest that processes within the confluence mixing zone change the concentrations of bioreactive solutes. DOM signatures at downstream sites were less aromatic and more amino acid-like than what would be predicted from conservative mixing, providing evidence for potential priming of more persistent OM metabolism in confluence mixing zones. Priming effects at confluences have been suggested in larger rivers with more divergent OM pools between tributaries and mainstem reaches (Ward et al., 2016; 2019). While the DOM signatures at our sites suggest a potential confluence OM priming effect, k_{DO} $pdiff_{DS}$ values showed that microbial respiration was both stimulated and suppressed downstream of confluences, indicating that confluence impacts on downstream biogeochemical processes are variable. By only considering net effects on biogeochemical patterns at the reach scale, we were unable to disentangle the possibility that the confluence mixing zone could function as both a source and a sink simultaneously for a given bioreactive parameter. Explicit measurements of biogeochemical processes within confluence mixing zones are needed to generate a more predictive framework that includes the mechanisms driving distinct biogeochemical patterns downstream of confluences. However, bioreactive parameters in the water column represent the cumulative effects of geomorphic, hydrologic, and biotic change downstream of confluences, and by detecting non-conservative mixing of bioreactive parameter downstream of confluences, we are confident that confluences do act as biogeochemical discontinuities within freshwater networks.

4.3 Reach- and Network-Scale Drivers Partially Explain Non-Conservative Mixing of Bioreactive Parameters

Non-conservative mixing of bioreactive parameters downstream of confluences was only partially explained by reach- and network-scale drivers. We observed

non-conservative mixing of all bioreactive parameters, however, $pdiff_{T:US}$ and $DA_T{:}DA_{US}$ both had low explanatory power of net source or sink dynamics for OM and nutrients. Confluences with comparatively small tributaries or tributaries with similar chemistry to the upstream reach still resulted in non-conservative mixing downstream of the confluence, showing that suggested network-scale predictors of biogeochemical patterns may not be applicable to confluences. Reach-scale drivers (w_{cv} and $\mathrm{WRT}_{100\mathrm{m}}$) did explain $k_{DO\text{-}reach}$ downstream of confluences; as geomorphic variability and residence times were positively related to rates of microbial respiration downstream of confluences. However, we observed the opposite trends between reach-scale drivers and $k_{DO\text{-}reach}$ downstream of confluences; w_{cv} and $\mathrm{WRT}_{100\mathrm{m}}$ were negatively related to rates of microbial respiration. Residence time has been shown to have an overall negative relationship with carbon metabolism along inland water continuums (Catalán et al., 2016), but a positive relationship with biogeochemical processes at freshwater ecosystem interfaces (Hampton et al., 2020; Zarnetske et al., 2011). The lack of explanatory power of network-scale drivers over biogeochemical patterns at confluences and the differences in trends between reach-scale drivers and $k_{DO\text{-}reach}$ suggests that confluences act as structural and functional discontinuities. As a result of confluence-specific geomorphic and hydrologic disturbances, the hierarchy of controls over biogeochemical processes within confluence mixing zones may differ from more traditional, continuum-based perspective of how streams transport and transform OM and nutrients.

While contributing reach chemistry and drainage area only partially explained non-conservative mixing of bioreactive parameters, there were observable links between biogeochemical patterns downstream of confluences and expectations of solute behavior in streams. DOC and NH_4-N were likely transport-limited at confluences given their low concentrations and the lack of explanatory power of both contributing reach chemistry and drainage area as drivers of downstream biogeochemical patterns (Covino, 2017). OM is often limited by hydrologic transport in streams (Zarnetske et al., 2018), which may be exacerbated downstream of confluences. Thermodynamic and stoichiometric favorability of OM and NH_4-N in NO_3-N rich environment may increase demand downstream of confluences (Helton et al., 2015). Non-conservative mixing and the net source dynamics of NO_3-N and SRP downstream of confluences were explained by positive relationships with both contributing reach chemistry and $DA_T{:}DA_{US}$. k_{DO} was suppressed downstream reaches of Con-1 and Con-2, which also were net sources of NO_3-N and SRP. Tributaries at Con-1 and Con-2 had high NO_3-N and SRP concentrations compared to their respective upstream reach. Steep hillslopes at Con-1 and Con-2 and the transition from intermittent flow upstream to permanent flow downstream of Con-1 suggests that these headwater confluences may act as points of flow accumulation and shallow subsurface flowpaths may influence biogeochemical patterns downstream. The positive relationships with contributing reach chemistry and $DA_T{:}DA_{US}$ suggests that NO_3-N and SRP are reaction-limited downstream of confluences and controlled by incoming fluxes over local changes within the mixing zone. However, SpC and Q measurements

at Con-1 and Con-2 do not allude to groundwater inputs in the confluence mixing zone. Additionally, biogeochemical processes such as nitrification could be stimulated in the confluence mixing zone and lead to a net increase NO_3-N (Zarnetske et al. 2011). Explicit measurements of how specific biogeochemical processes are altered within confluence mixing zones are needed to further explain the discrepancy between predicted and observed biogeochemical patterns downstream.

Biogeochemical patterns and non-conservative mixing of bioreactive parameters downstream of confluences could change as a function of flow, season, or other environmental drivers. We observed differences in OM and nutrient chemistry between summer and fall, as well as seasonal differences in non-conservative mixing downstream of confluences. Depending on the time of year and flow conditions, biogeochemical patterns downstream of confluences may be dominated by a single source or a mixture of several upstream sources. Changes in temperature, both temporally and spatially, can impact how water and materials mix downstream of confluences (Lewis & Rhoads, 2015), as well as drive potential changes in in-stream biogeochemical processes. Differences in canopy cover at a confluence may increase the light available to fuel in-stream production (Bernhardt et al., 2022). Differences in pH between tributary and upstream reaches can also drive changes in metal speciation downstream of confluences and may act as an additional control over reach-scale patterns in bioreactive parameters downstream of confluences (Schemel et al., 2000). Understanding the relevant controls and scales of influences that drive biogeochemical processes downstream of confluences is needed to provide explanation to the non-conservative mixing patterns we observed in this study.

Conclusions

Confluences are fundamental to river network structure and the potential for confluences to act as unique sites of biogeochemical processing highlights the need to understand how confluences impact ecosystem structure and function throughout freshwater networks. We found that confluences act as geomorphic and biogeochemical discontinuities along mainstem reaches and that biogeochemical patterns downstream of confluences could not be explained through conservative mixing of upstream and tributary reaches alone. Non-conservative mixing responses downstream of confluences were variable among confluences and only partially explained by differences in contributing reach chemistry and drainage area. Explicit measurements of biogeochemical processes across above, below, and within the confluence mixing zone are needed to further elucidate the relative importance of watershed- and reach-scale controls over non-conservative mixing at confluences. Based on our results, we recommend further investigation into the spatial heterogeneity within confluence mixing zones, the influence of flow and seasonality on non-conservative mixing patterns downstream of confluences, and the underlying mechanisms and hierarchy of controls behind confluence-driven alterations to biogeochemical cycles. Together, our findings of non-conservative mixing of bioreactive parameters downstream of confluences

contradict assumptions of linear scaling made in network models for DOC and nutrient transport (Bertuzzo et al., 2017; Helton et al., 2018). Ignoring the types of confluence effects on downstream geomorphology, hydrology, and biogeochemistry that we have observed in this study would have cascading effects on network-scale water quality assessments and management of freshwater resources. Understanding the mechanisms behind confluence-driven alterations to biogeochemical cycles is needed to generate a predictive framework for how confluences and other discontinuities alter ecosystem structure and function throughout freshwater networks.

Acknowledgements

This work was supported by the National Science Foundation (DEB-1754237 to ERH and DGE-1840995 to SP), and a Virginia Tech Integrative and Innovative Solutions for Freshwater Systems Seed Grant to ERH, DTS, and SP. We would like to thank Katherine Pérez Rivera, Carla López Lloreda, Kristen Bretz, Felicity deToll, Morgan Wood, Katherine Wardinski, Sophie Drew, Adrienne Breef-Pilz, Alaina Weinheimer, Tadhg Moore, Cameron Braswell, and Kelly Crum for their assistance during the sampling campaigns. Many thanks to Bobbie Niederlehner, Alexandra Hounshell, and Kelly Peeler for their assistance with analytical chemistry as well as Erich Hester and Jeb Barrett for their feedback on this work.

Data Availability Statement

Data, code, and supplemental materials are publicly available through HydroShare at: http://www.hydroshare.org/resource/c5e687fa040e4707ba922002bafd18fd

References

Abarca, M., Guerra, P., Arce, G., Montecinos, M., Escauriaza, C., Coquery, M., & Pastén, P. (2017). Response of suspended sediment particle size distributions to changes in water chemistry at an Andean mountain stream confluence receiving arsenic rich acid drainage. *Hydrological Processes*, 31(2), 296–307. https://doi.org/10.1002/hyp.10995

Abbott, B. W., Baranov, V., Mendoza-Lera, C., Nikolakopoulou, M., Harjung, A., Kolbe, T., et al. (2016). Using multi-tracer inference to move beyond single-catchment ecohydrology. *Earth-Science Reviews*, 16, 19–42. https://doi.org/10.1016/j.earscirev.2016.06.014

Abbott, B. W., Gruau, G., Zarnetske, J. P., Moatar, F., Barbe, L., Thomas, Z., et al. (2018). Unexpected spatial stability of water chemistry in headwater stream networks. *Ecology Letters*, 21(2), 296–308. https://doi.org/10.1111/ele.12897

APHA. (1998). *Standard methods for the examination of water and wastewater* (20th ed.). American Public Health Association.

Benda, L., Andras, K., Miller, D., & Bigelow, P. (2004). Confluence effects in rivers: Interactions of basin scale, network geometry, and disturbance regimes.

Water Resources Research, 40(5), 1–15. https://doi.org/10.1029/2003wr002583

Benda, L., Poff, N. L., Miller, D., Dunne, T., Reeves, G., Pess, G., & Pollock, M. (2004). The Network Dynamics Hypothesis: How Channel Networks Structure Riverine Habitats. *BioScience*, 54(5), 413–427. https://doi.org/10.1641/0006-3568(2004)054[0413:TNDHHC]2.0.CO;2

Bernhardt, E. S., Blaszczak, J. R., Ficken, C. D., Fork, M. L., Kaiser, K. E., & Seybold, E. C. (2017). Control Points in Ecosystems: Moving Beyond the Hot Spot Hot Moment Concept. *Ecosystems*, 20(4), 665–682. https://doi.org/10.1007/s10021-016-0103-y

Bernhardt, E. S., Savoy, P., Vlah, M. J., Appling, A. P, Koenig, L. E., Hall Jr., R. O., et al. (2022). Light and flow regimes regulate the metabolism of rivers. *Proceedings of the National Academy of Sciences*, 119(8), e2121976119. https://doi.org/10.1073/pnas.2121976119

Bertuzzo, E., Helton, A. M., Hall, R. O., Jr., & Battin, T. J. (2017). Scaling of dissolved organic carbon removal in river networks. *Advances in Water Resources*, 110, 136–146. https://doi.org/10.1016/j.advwatres.2017.10.009

Best, J. L. (1988). Sediment transport and bed morphology at river channel confluences. *Sedimentology*, 35, 481-498. https://doi.org/10.1111/j.1365-3091.1988.tb00999.x.

Catalán, N., Marcé, R., Kothawala, D. N., & Tranvik, L. J. (2016). Organic carbon decomposition rates controlled by water retention time across inland waters. *Nature Geoscience*, 9(7), 501–504. https://doi.org/10.1038/ngeo2720

Coble, P. G. (1996). Characterization of marine and terrestrial DOM in seawater using excitation-emission matrix spectroscopy. *Marine Chemistry*, 51(4), 325–346. https://doi.org/10.1016/0304-4203(95)00062-3

Cory, R. M., Miller, M. P., McKnight, D. M., Guerard, J. J., & Miller, P. L. (2010). Effect of instrument-specific response on the analysis of fulvic acid fluorescence spectra. *Limnology & Oceanography: Methods*, 8, 67–78. https://doi.org/10.4319/lom.2010.8.67

Covino, T. (2017). Hydrologic connectivity as a framework for understanding biogeochemical flux through watersheds and along fluvial networks. *Geomorphology*, 277, 133–144. https://doi.org/10.1016/j.geomorph.2016.09.030

Creed, I. F., McKnight, D. M., Pellerin, B. A., Green, M. B., Bergamaschi, B. A., Aiken, G. R., et al. (2015). The river as a chemostat: fresh perspectives on dissolved organic matter flowing down the river continuum. *Canadian Journal of Fisheries and Aquatic Sciences*, 72, 1272–1285. https://doi.org/10.1139/cjfas-2014-0400

Ensign, S. H., & Doyle, M. W. (2006). Nutrient spiraling in streams and river networks. Journal of Geophysical Research, 111, G04009. https://doi.org/10.1029/2005JG000114

Environmental Systems Research Institute, (2022). ArcGIS Desktop Help 10.7 Geostatistical Analyst. Retrieved from http://resources.arcgis.com/en/help/main/10.2/index.html

Farjalla, V. F. (2014). Are the mixing zones between aquatic ecosystems hot spots of bacterial production in the Amazon River system? *Hydrobiologia*, 728(1), 153–165. https://doi.org/10.1007/s10750-014-1814-8

Fernandes, C. C., Podos, J., & Lundberg, J. G. (2004). Amazonian ecology: tributaries enhance the diversity of electric fishes. *Science*, 305(5692), 1960–1962. https://doi.org/10.1126/science.1101240

Fisher, S. G., Sponseller, R. A., & Heffernan, J. B. (2004). Horizons in stream biogeochemistry: Flowpaths to progress. *Ecology*, 85(9), 2369–2379. https://doi.org/10.1890/03-0244

Gaudet, J. M., & Roy, A. G. (1995). Effect of bed morphology on flow mixing length at river confluences. *Nature*, 373(6510), 138–139. https://doi.org/10.1038/373138a0

Gelman, A., & Rubin, D. B. (1992). Inference from Iterative Simulation Using Multiple Sequences. *Statistical Science*, 7(4), 457–472.

Hampton, T. B., Zarnetske, J. P., Briggs, M. A., Dehkordy, F. M. P., Singha, K., Day-Lewis, F. D., et al. (2020). Experimental shifts of hydrologic residence time in a sandy urban stream sediment–water interface alter nitrate removal and nitrous oxide fluxes. *Biogeochemistry* 149, 195–219. https://doi.org/10.1007/s10533-020-00674-7

Harvey, J., & Gooseff, M. (2015). River corridor science: Hydrologic exchange and ecological consequences from bedforms to basins. *Water Resources Research*, 51, 6893–6922. https://doi.org/10.1002/2015WR017617

Helton, A. M., Hall Jr., R. O., & Bertuzzo, E. (2018). How network structure can affect nitrogen removal by streams. *Freshwater Biology*, 63, 128–140. https://doi.org/10.1111/fwb.12990

Helton, Ashley M., Ardón, M., & Bernhardt, E. S. (2015). Thermodynamic constraints on the utility of ecological stoichiometry for explaining global biogeochemical patterns. *Ecology Letters*, 18(10), 1049–1056. https://doi.org/10.1111/ele.12487

Hotchkiss, E. R., Hall Jr., R. O., Baker, M. A., Rosi-Marshall, E. J., & Tank, J.L. (2014). Modeling priming effects on microbial consumption of dissolved organic carbon in rivers. *Journal of Geophysical Research Biogeosciences.*, 119, 982– 995. https://doi.org/10.1002/2013JG002599

Hynes, H. B. N. (1975). The stream and its valley. *SIL Proceedings, 1922-2010*, 19(1), 1–15. https://doi.org/10.1080/03680770.1974.11896033

Kiffney, P. M., Greene, C. M., Hall, J. E., & Davies, J. R. (2006). Tributary streams create spatial discontinuities in habitat, biological productivity, and di-

versity in mainstem rivers. *Canadian Journal of Fisheries and Aquatic Sciences*, 63(11), 2518–2530. https://doi.org/10.1139/f06-138

Koenig, L. E., Helton, A. M., Savoy, P., Bertuzzo, E., Heffernan, J. B., Hall Jr, R. O., & Bernhardt, E. S. (2019). Emergent productivity regimes of river networks. *Limnology & Oceanography: Letters*, 4, 173–181. https://doi.org/10.1002/lol2.10115

Krause, S., Lewandowski, J., Grimm, N. B., Hannah, D. M., Pinay, G., McDonald, K., et al. (2017). Ecohydrological interfaces as hot spots of ecosystem processes. *Water Resources Research*, 53, 6359–6376. https://doi.org/10.1002/2016WR019516

Lewis, Q. W., & Rhoads, B. L. (2015). Rates and patterns of thermal mixing at a small stream confluence under variable incoming flow conditions. *Hydrological Processes*, 29, 4442– 4456. https://doi.org/10.1002/hyp.10496

Mansour, I., Heppell, C. M., Ryo, M., & Rillig, M. C. (2018). Application of the microbial community coalescence concept to riverine networks. *Biological Reviews*, 93(4), 1832– 1845. https://doi.org/10.1111/brv.12422

McGuire, K. J., Torgersen, C. E., Likens, G. E., Buso, D. C., Lowe, W. H., & Bailey, S. W. (2014). Network analysis reveals multiscale controls on streamwater chemistry. *Proceedings of the National Academy of Sciences*, 111(19), 7030–7035. https://doi.org/10.1073/pnas.1404820111

Mulholland, P. J., Helton, A. M., Poole, G. C., Hall, R. O., Hamilton, S. K., Peterson, B. J., et al. (2008). Stream denitrification across biomes and its response to anthropogenic nitrate loading. *Nature*, 452(7184), 202–205. https://doi.org/10.1038/nature06686

Murphy, J., & Riley, J. P. (1962). A modified single solution method for the determination of phosphate in natural waters. *Analytica Chimica Acta*, *27*, 31–36. https://doi.org/10.1016/s0003-2670(00)88444-5

Plont, S., Riney, J., & Hotchkiss, E. R. (2022). Integrating perspectives on dissolved organic carbon removal and whole-stream metabolism. *Journal of Geophysical Research Biogeosciences*, 127, e2021JG006610. https://doi.org/10.1029/2021JG006610

Poole, G. C. (2002). Fluvial landscape ecology: addressing uniqueness within the river discontinuum. *Freshwater Biology*, 47(4), 641–660. https://doi.org/10.1046/j.1365- 2427.2002.00922.x

Raymond, P. A., Saiers, J. E., & Sobczak, W. V. (2016). Hydrological and biogeochemical controls on watershed dissolved organic matter transport: pulse-shunt concept. *Ecology*, 97(1), 5–16. https://doi.org/10.1890/14-1684.1

Rhoads, B. L., & Kenworthy, S. T. (1998). Time-averaged flow structure in the central region of a stream confluence. *Earth Surface Processes and Landforms*, 23, 171–191. https://doi.org/10.1002/(SICI)1096-9837(199802)23:2<171::AID-ESP842>3.0.CO;2-Rhoads, B. L. (1987). Changes in stream channel

characteristics at tributary junctions. *Physical Geography*, 8(4), 346–361. https://doi.org/10.1080/02723646.1987.10642333

Rice, S. P., Greenwood, M. T., & Joyce, C. B. (2001). Tributaries, sediment sources, and the longitudinal organisation of macroinvertebrate fauna along river systems. *Canadian Journal of Fisheries and Aquatic Sciences*, 58, 824–840. https://doi.org/10.1139/f01-022

Rice, S. P. (2017). Tributary connectivity, confluence aggradation and network biodiversity. *Geomorphology*, 277, 6–16. https://doi.org/10.1016/j.geomorph.2016.03.027

R Core Team. (2022). *R: A language and environment for statistical computing*. R Foundation for Statistical Computing. Retrieved from http://www.R-project.org/

Schemel, L. E., Kimball, B. A., & Bencala, K. E. (2000). Colloid formation and metal transport through two mixing zones affected by acid mine drainage near Silverton, Colorado. *Applied Geochemistry*, 15, 1003–1018. https://doi.org/10.1016/S0883-2927(99)00104-3

Schemel, L. E., Cox, M. H., Runkel, R. L., & Kimball, B. A. (2006). Multiple injected and natural conservative tracers quantify mixing in a stream confluence affected by acid mine drainage near Silverton, Colorado. *Hydrological Processes*, 20(13), 2727–2743. https://doi.org/10.1002/hyp.6081

Schmadel, N. M., Ward, A. S., Lowry, C. S., & Malzone, J. M. (2016). Hyporheic exchange controlled by dynamic hydrologic boundary conditions. *Geophysical Research Letters*, 43(9), 4408–4417. https://doi.org/10.1002/2016GL068286

Shogren, A. J., Zarnetske, J. P., Abbott, B. W., Bratsman, S., Brown, B., Carey, M. P., et al. (2022). Multi-year, spatially extensive, watershed-scale synoptic stream chemistry and water quality conditions for six permafrost-underlain Arctic watersheds. *Earth System Science Data*, 14(1), 95–116. https://doi.org/10.5194/essd-14-95-2022

Solorzano, L. (1969). Determination of ammonia in natural water by the phenolhypochlorite method. *Limnology & Oceanography*, 14(5), 799–801. https://doi.org/10.4319/lo.1969.14.5.0799

Stedmon, C. A., & Bro, R. (2008). Characterizing dissolved organic matter fluorescence with parallel factor analysis: a tutorial. *Limnology & Oceanography: Methods*, 6, 572–579. https://doi.org/10.4319/lom.2008.6.572

U.S. Geological Survey, 2014, National Land Cover Database (NLCD) 2011 Land Cover Conterminous United States: U.S. Geological Survey data release, https://doi.org/10.5066/P97S2IID

U.S. Geological Survey. (2019). *Virginia FEMA NRCS South Central lidar project*. Dewberry.

Vannote, R. L., Minshall, G. W., Cummins, K. W., Sedell, J. R., & Cushing, C. E. (1980). The River Continuum Concept. *Canadian Journal of Fisheries and*

Aquatic Sciences, 37(1), 130–137. https://doi.org/10.1139/f80-017

Ward, A. S., Fitzgerald, M., Gooseff, M. N., Voltz, T. J., Binley, A. M., & Singha, K. (2012). Hydrologic and geomorphic controls on hyporheic exchange during base flow recession in a headwater mountain stream. *Water Resources Research*, 48, W04513. https://doi.org/10.1029/2011WR011461

Ward, N. D., Bianchi, T. S., Sawakuchi, H. O., Gagne-Maynard, W., Cunha, A. C., Brito, D. C., et al. (2016). The reactivity of plant-derived organic matter and the potential importance of priming effects along the lower Amazon River. *Journal of Geophysical Research Biogeosciences*, 121(6), 1522–1539. https://doi.org/10.1002/2016JG003342

Ward, N. D., Sawakuchi, H. O., Richey, J. E., Keil, R. G., Bianchi, T. S., & Lehrter, J. C. (2019). Enhanced aquatic respiration associated with mixing of clearwater tributary and turbid Amazon River waters. *Frontiers of Earth Science*, 7, 1–6. https://doi.org/10.3389/feart.2019.00101

Weishaar, J. L., Aiken, G. R., Bergamaschi, B. A., Fram, M. S., Fujii, R., & Mopper, K. (2003). Evaluation of Specific Ultraviolet Absorbance as an Indicator of the Chemical Composition and Reactivity of Dissolved Organic Carbon. *Environmental Science & Technology*, 37(20), 4702–4708. https://doi.org/10.1021/es030360x

Wipfli, M. S., & Gregovich, D. P. (2002). Export of invertebrates and detritus from fishless headwater streams in southeastern Alaska: implications for downstream salmonid production. *Freshwater Biology*, 47(5), 957–969. https://doi.org/10.1046/j.1365- 2427.2002.00826.x

Zarnetske, J. P., Haggerty, R., Wondzell, S. M., & Baker, M. A. (2011). Dynamics of nitrate production and removal as a function of residence time in the hyporheic zone. *Journal of Geophysical Research*, 116, G01025. https://doi.org/10.1029/2010jg001356

Zarnetske, J. P., Bouda, M., Abbott, B. W., Saiers, J., & Raymond, P. A. (2018). Generality of hydrologic transport limitation of watershed organic carbon flux across ecoregions of the United States. *Geophysical Research Letters*, 45(21), 11,702-11,711. https://doi.org/10.1029/2018GL080005

Table of Contents

Note: Data and code used in the analyses of this manuscript are available at: http://www.hydroshare.org/resource/c5e687fa040e4707ba922002bafd18fd

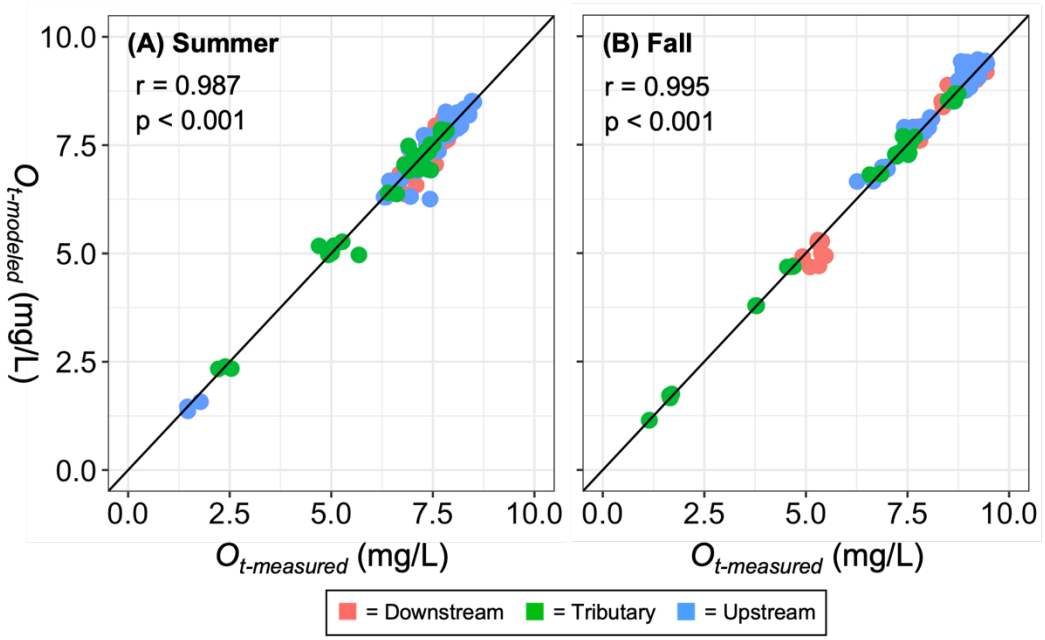

Supplementary Figure 1: Modeled final dissolved oxygen concentration based on water column microbial respiration rates ($O_{t\text{-}modeled}$, mg/L) versus measured final dissolved oxygen concentration ($O_{t\text{-}measured}$, mg/L) for all summer (A) and fall (B) microbial respiration assays. Black lines represent $O_{t\text{-}modeled} = O_{t\text{-}measured}$. Pearson correlation coefficients (r) and p-values are included for both summer and fall results. Microbial respiration assays conducted in downstream, tributary, and upstream reaches of a confluence are represented by different colors.

Supplementary Table 1: Two-way ANOVA p-values for specific conductivity (SpC), microbial respiration rate (k_{DO}), dissolved organic carbon (DOC), specific ultraviolet absorbance at 254 nm ($SUVA_{254}$), peak C (C), peak T (T), peak C: peak T (C:T), ammonium (NH_4-N), nitrate (NO_3-N), and soluble reactive phosphorus (SRP) for each confluence. Season (summer vs. fall) and reach (US vs. DS) were treated as fixed effects. For all tests, we assigned a significance level of $p < 0.05$. Significant results are bolded. Significant interactions were interpreted as differences in upstream vs. downstream parameter values were seasonally-dependent.

Parameter	Comparison	Con-1	Con-2	Con-3	Con-4	Con-5
SpC	Su vs. F	**<0.001**	**<0.001**	**<0.001**	**<0.001**	**<0.001**
	US vs. DS	0.078	**<0.001**	**<0.001**	**<0.001**	0.051
	Interaction	0.115	**<0.001**	0.075	**<0.001**	0.874
k_{DO}	Su vs. F	0.286	**0.005**	0.714	0.289	0.246
	US vs. DS	**0.016**	0.103	0.248	0.487	0.279
	Interaction	**<0.001**	0.135	0.813	0.898	**0.018**
DOC	Su vs. F	**0.006**	**<0.001**	**<0.001**	**<0.001**	0.060
	US vs. DS	0.688	0.973	0.255	**0.014**	0.380
	Interaction	0.835	0.678	0.283	0.220	0.055
$SUVA_{254}$	Su vs. F	0.135	**0.018**	0.380	**<0.001**	**<0.001**
	US vs. DS	0.293	**0.019**	0.202	**0.008**	0.485
	Interaction	0.544	**0.017**	0.167	**0.028**	0.269
C	Su vs. F	0.068	**0.002**	**<0.001**	0.055	**<0.001**
	US vs. DS	0.180	0.575	**0.007**	0.678	0.366
	Interaction	0.323	0.707	**0.002**	**0.025**	**<0.001**
T	Su vs. F	**0.002**	**<0.001**	**<0.001**	**0.001**	**<0.001**
	US vs. DS	**0.031**	0.148	0.634	0.659	**0.021**
	Interaction	**0.009**	**0.009**	0.096	0.244	0.078
C:T	Su vs. F	**0.044**	0.068	0.229	**0.011**	**<0.001**
	US vs. DS	0.268	0.094	**0.013**	0.885	0.155
	Interaction	0.220	0.064	**0.001**	0.058	**<0.001**
NH_4-N	Su vs. F	**0.038**	0.179	**<0.001**	**0.017**	**0.004**
	US vs. DS	0.894	0.884	**0.021**	0.278	0.314
	Interaction	0.360	0.058	0.062	0.211	0.157
NO_3-N	Su vs. F	**<0.001**	**0.009**	**<0.001**	**<0.001**	**<0.001**
	US vs. DS	**0.001**	**<0.001**	**0.011**	0.656	0.144
	Interaction	**0.002**	0.091	0.526	0.079	0.340
SRP	Su vs. F	0.116	**0.023**	**<0.001**	**<0.001**	**<0.001**
	US vs. DS	0.215	0.618	0.413	**<0.001**	0.691
	Interaction	0.379	**0.031**	0.841	**<0.001**	0.732

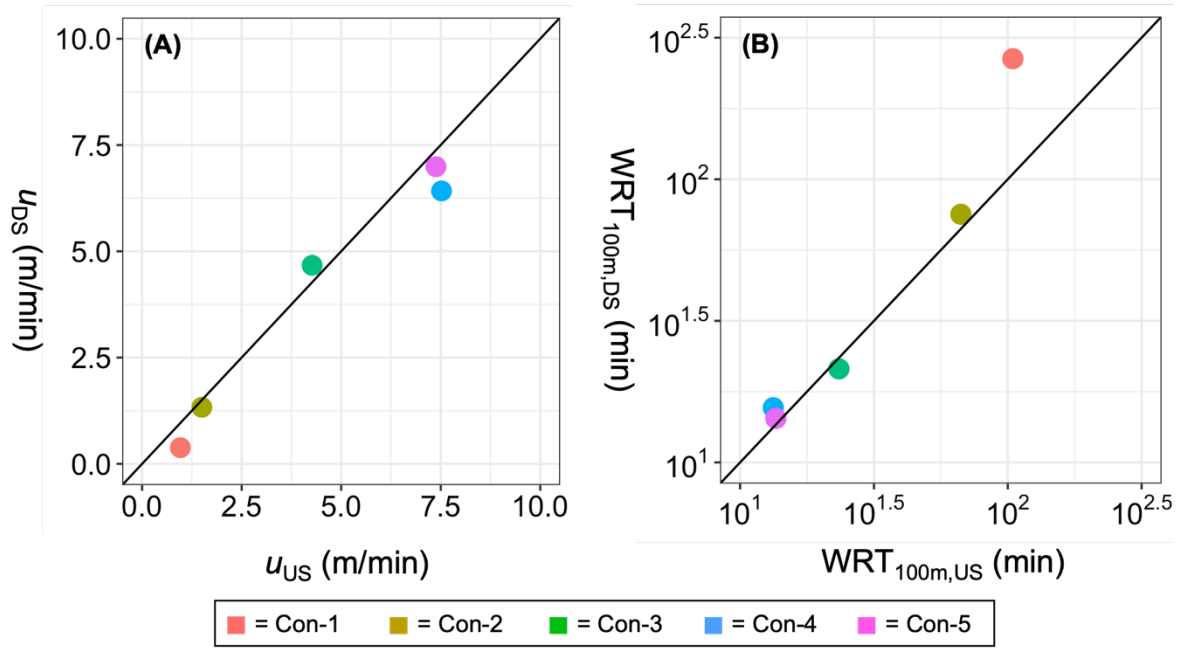

Supplementary Figure 2: Downstream reach-scale velocity (u_{DS}, m/min) versus upstream reach-scale velocity (u_{US}, m/min; A) and downstream water residence time normalized to a 100 meter reach ($WRT_{100m,DS}$, min) versus upstream water residence time normalized to a 100 meter reach ($WRT_{100m,US}$, min; B). Black lines are 1:1 line for downstream and upstream u and WRT_{100m}, respectively. Each confluence is represented by a different color.

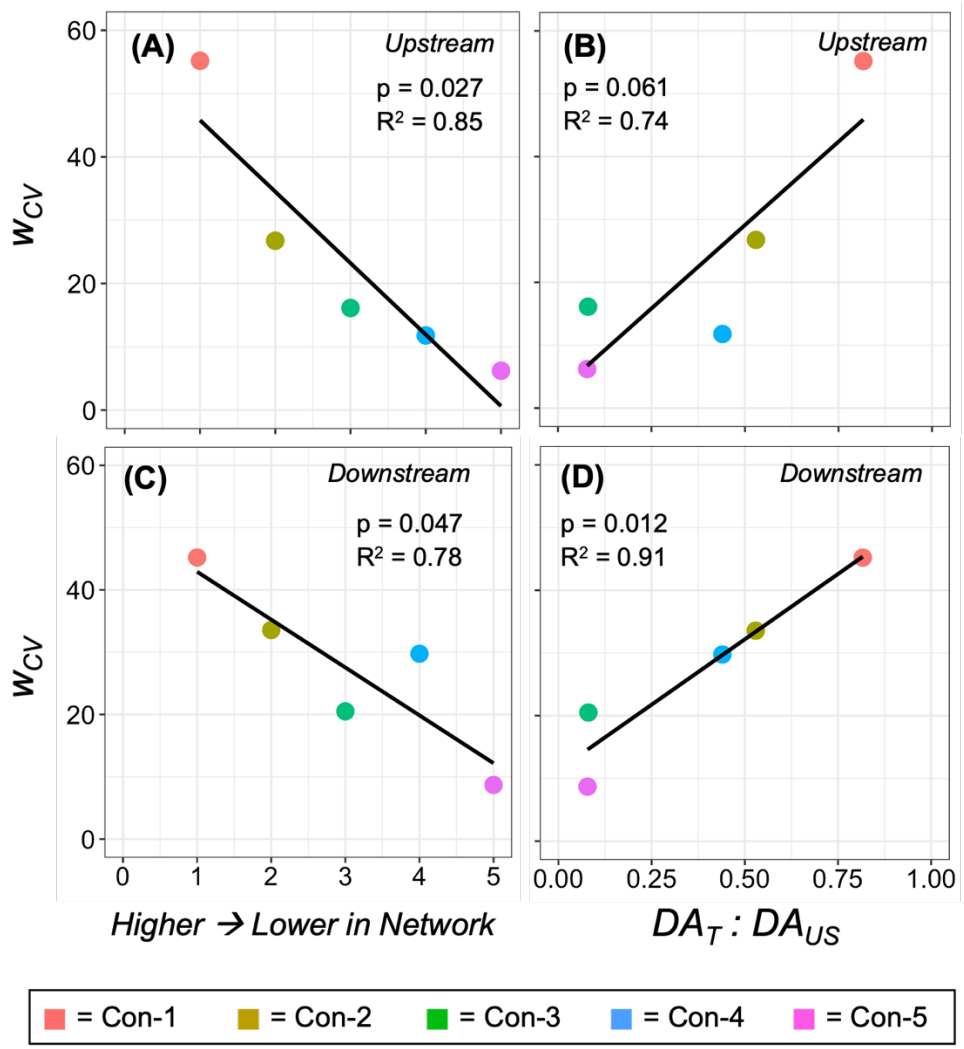

Supplementary Figure 3: Reach-scale coefficient of variation for wetted width (w_{cv}) versus confluence position in the network (A for upstream reaches, C for downstream reaches) and w_{cv} versus the ratio of tributary (T) and upstream (US) watershed drainage areas (DA_T:DA_{US}; B for upstream reaches, D for downstream reaches) for each confluence. Each confluence is represented by a different color. Black lines are linear fits of the data. R^2 values from simple linear regressions are included for all parameters.